NASA TECHNICAL NOTE

NASA TN D-5590

c. 1

NASA TN D-5590

AN AUTOMATIC RESTART CONTROL SYSTEM FOR AN AXISYMMETRIC MIXED-COMPRESSION INLET

by Gary L. Cole, George H. Neiner, and Michael J. Crosby

Lewis Research Center
Cleveland, Ohio

NATIONAL AERONAUTICS AND SPACE ADMINISTRATION • WASHINGTON, D. C. • DECEMBER 1969

1. Report No.	2. Government Accession No.	3. Recipient's Catalog No.
NASA TN D-5590		

4. Title and Subtitle	5. Report Date
AN AUTOMATIC RESTART CONTROL SYSTEM FOR AN AXISYMMETRIC MIXED-COMPRESSION INLET	December 1969
	6. Performing Organization Code
7. Author(s) Gary L. Cole, George H. Neiner, and Michael J. Crosby	8. Performing Organization Report No. E-5219
9. Performing Organization Name and Address: Lewis Research Center, National Aeronautics and Space Administration, Cleveland, Ohio 44135	10. Work Unit No. 720-03
	11. Contract or Grant No.
12. Sponsoring Agency Name and Address: National Aeronautics and Space Administration, Washington, D.C. 20546	13. Type of Report and Period Covered: Technical Note
	14. Sponsoring Agency Code

15. Supplementary Notes

16. Abstract

An automatic restart control system is described which, unlike conventional inlet controls, retains closed-loop control of terminal shock position throughout a restart cycle. Closed-loop terminal shock control is retained so that near maximum diffuser-exit pressure recovery and minimum distortion levels can be achieved. The restart control system was tested with the inlet coupled alternately to a cold pipe having a choked-exit plug and a J85-13 turbojet engine. Tests were conducted in the Lewis 10- by 10-Foot Supersonic Wind Tunnel at free-stream Mach numbers of 2.50, 2.30, and 2.02. The inlet was unstarted by a downstream disturbance and, in all cases, the inlet was successfully restarted.

17. Key Words (*Suggested by Author(s)*)	18. Distribution Statement
Intake systems Supersonic inlets Shock wave control Control Restart control	Unclassified - unlimited

19. Security Classif. (of this report)	20. Security Classif. (of this page)	21. No. of Pages	22. Price*
Unclassified	Unclassified	39	$3.00

*For sale by the Clearinghouse for Federal Scientific and Technical Information
Springfield, Virginia 22151

AN AUTOMATIC RESTART CONTROL SYSTEM FOR AN AXISYMMETRIC MIXED-COMPRESSION INLET

by Gary L. Cole, George H. Neiner, and Michael J. Crosby

Lewis Research Center

SUMMARY

The objective of the investigation was to develop a restart control system which, unlike conventional inlet controls, would retain closed-loop control of terminal shock position during the restart cycle. This objective was achieved. The advantage of retaining terminal shock control during the restart cycle is that near maximum diffuser-exit pressure recovery can be achieved. Such a system also minimizes distortion at the diffuser exit.

The control signal used to sense when the inlet was unstarted was the ratio of a static pressure just aft of the cowl lip to a throat total pressure. Inlet restart was accomplished by translating the inlet centerbody forward to increase the throat-to-capture area ratio.

The terminal shock control feedback signal was a throat-exit static pressure, and the overboard bypass door area was the manipulated variable. It was necessary to schedule the terminal shock control command as a function of centerbody position. No attempt was made to find control signals that were valid for the entire operating range of the inlet.

The restart control system was tested in the Lewis 10- by 10-Foot Supersonic Wind Tunnel on a Mach 2.5 design axisymmetric, mixed-compression inlet. Tests were conducted with the inlet coupled alternately to a cold pipe having a choked-exit plug and a J85-13 turbojet engine. Tests were made at Mach 2.50, 2.30 (cold pipe only), and 2.02. A downstream airflow disturbance was used to unstart the inlet. In all cases, the restart control successfully restarted the inlet. The restart cycle took approximately 1.4, 1.0, and 0.5 second at free-stream Mach numbers of 2.50, 2.30, and 2.02, respectively. The restart cycle time was dependent on the centerbody travel required to restart the inlet and the maximum slewing velocity of the centerbody servo.

INTRODUCTION

The basic function of a supersonic inlet is to provide an engine with air at those levels of pressure and velocity required by the engine. In a mixed-compression inlet, this is usually accomplished by maintaining the terminal shock just downstream of the aerodynamic throat. This type of operation generally minimizes distortion of the airflow and maximizes pressure recovery at the diffuser exit. If a disturbance in the flow displaces the terminal shock to a point upstream of the aerodynamic throat, the shock becomes unstable and is expelled from the inlet. This phenomenon, known as an inlet unstart, results in a large loss in pressure recovery and often an increase in airflow distortion at the diffuser exit or compressor-face station. Distortion in this context refers to a spatial asymmetry of pressure at the compressor-face station. After unstart, the shock may be stationary indicating that the inlet is in a stable-unstarted condition. If the shock exhibits an oscillatory motion after unstart, the inlet is in an unstable-unstarted condition known as buzz. If buzz occurs, there are large fluctuations in pressure throughout the inlet. Some consequences that may result from these conditions are degradation of engine performance, combustor blowout, compressor stall, or structural fatigue of the engine's compressor blades and the inlet structure.

An ideal terminal shock control would eliminate the possibility of an inlet unstart. Since this is not attainable with present control systems, the inlet control must have the additional capability of restarting the inlet in the event of an unstart.

Present restart control systems for mixed-compression inlets disable the terminal shock control and open the bypass doors to a fixed area upon sensing an inlet unstart. Generally, mixed-compression inlets are unstable when an unstart occurs, and opening the bypass doors will stabilize the inlet by choking the throat. Concurrently, the inlet throat-to-capture area ratio is increased until the shock is reswallowed. Then the throat-to-capture area is decreased to the design value. The terminal shock control is reactivated some time after the inlet is restarted.

During normal, started operation of mixed-compression inlets, variations in engine airflow are generally compensated for by the overboard bypass system. In this manner, the terminal shock can be positioned such that the best inlet performance is maintained. If the bypass doors are scheduled to open upon unstart, the scheduled area must be large enough to compensate for the maximum reduction in engine airflow that could occur as a result of the unstart. However, scheduling bypass area for a bypass flow greater than that required would result in higher distortion and lower pressure recovery than are potentially attainable. If the engine continues to operate normally after the unstart transient, the increase in distortion could initiate a compressor stall. It would therefore be desirable to position the bypass doors automatically to optimize conditions at the compressor-face station.

This report describes the investigation of a restart control which retains terminal shock control during the entire restart cycle. The control was tested on a Mach 2.5 mixed-compression inlet. Tests were conducted in the Lewis 10- by 10-Foot Supersonic Wind Tunnel at free-stream Mach numbers of 2.50, 2.30, and 2.02. During the test program, the inlet was terminated by either a cold pipe with choked-exit plug or a J85-13 engine.

APPARATUS AND PROCEDURE

The inlet used for the investigation was an axisymmetric mixed-compression type with 60 percent of the supersonic area contraction occurring internally at the design Mach number of 2.5. An isometric view of the inlet is displayed in figure 1.

The inlet was sized to match the J85-13 engine corrected airflow requirements of 15.83 kilograms per second at the design Mach number of 2.50, a free-stream temperature of 390 K, and a total pressure recovery of 90 percent. The inlet capture area was 1760 square centimeters. Additional aerodynamic design details of the inlet are described in references 1 and 2.

The inlet was attached to a cylindrical nacelle 63.5 centimeters in diameter in which either a cold pipe with a variable area choked-exit plug or a J85-13 engine could be installed. Both were used during the test program. The J85-13 engine that was used had a first-stage turbine stator flow area of 230 square centimeters - or 86 percent of the standard area. The stator had been altered for a previous test program to allow the compressor to be stalled without causing the engine exhaust gas temperature limit to be exceeded.

The inlet was equipped with a translating centerbody, six high-response sliding plate overboard bypass doors, and an ejector bypass, which are shown in figure 2(a). The translating centerbody was used to vary the inlet throat area. The ejector bypass was used for engine cooling (approx. 3 percent of the inlet mass flow). The bypass doors were located symmetrically around the inlet just upstream of the compressor-face station. They were used to match inlet airflow to engine airflow requirements and were capable of bypassing approximately 88 percent of the design inlet capture airflow. The overboard bypass system was designed to allow the inlet to operate on design with the engine passing no airflow. Both the ejector bypass and the overboard bypass exits were choked. The centerbody and each bypass door could be controlled independently by means of individual electrohydraulic servomechanisms.

Steady-state performance of the inlet and additional design details of the overboard bypass and ejector bypass systems are given in reference 2. The dynamic response of the

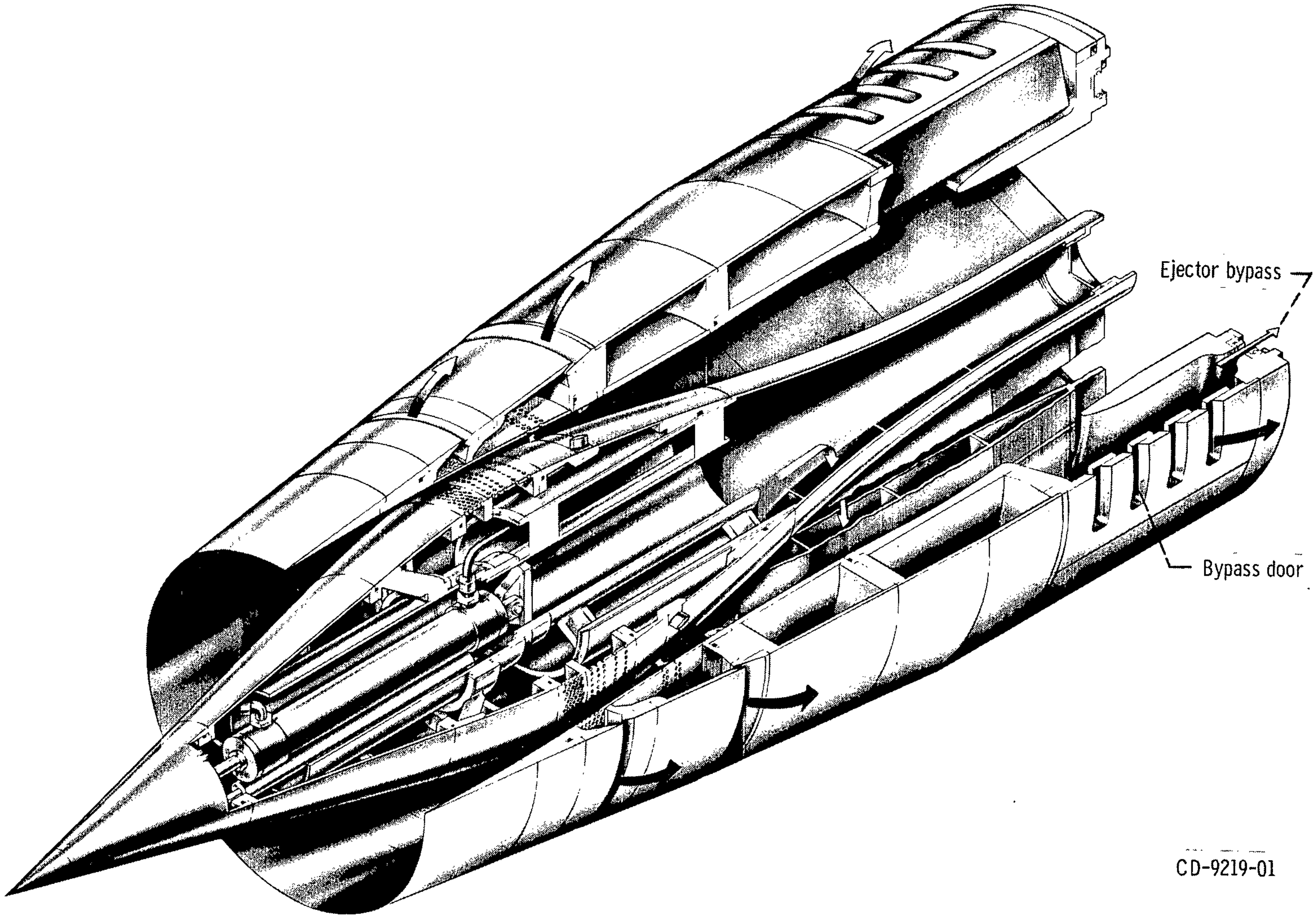

Figure 1. - Isometric view of inlet

inlet to flow disturbances, both upstream and downstream of the terminal shock, is described in reference 3.

Porous bleed regions were located on the cowl and centerbody surfaces both forward and aft of the inlet geometric throat. One bleed configuration was used during tests with the cold pipe, and another during tests with the engine. The bleed configurations that were used are shown in figure 2(b). It can be seen that the aft bleed was blocked during engine tests. This was done so that the inlet could be unstarted over a wider range of engine speeds.

Vortex generators were used on the centerbody during cold-pipe tests. During tests with the engine, vortex generators were also used on the cowl to help reduce distortion at the diffuser exit. The locations of the vortex generators are shown in figure 2(a).

Figures 2(a) and (c) show the axial location and arrangement of rakes used to measure steady-state total pressure recovery and distortion. Total pressure recovery H_2/H_0 (all symbols defined in the appendix) was computed as an area weighted average of rakes 1 to 6 (fig. 2(c)), located at station 2 just upstream of the compressor face. Additional measurements (rakes 7 to 10) were included in the calculation of the quantity (H_{max} - H_{min}), which was used to calculate distortion.

Figure 2(d) shows the locations of close coupled dynamic pressure transducers that were used for data and control. Static pressure measurements are indicated by solid circles while total-pressure measurements are denoted by open circles. The frequency response of each transducer and its coupled line was flat within 0 to +3 decibels to approximately 250 hertz. The signals that were used for control were a static pressure just aft of the cowl lip P_{cl}, a throat total pressure H_{th}, a throat-exit static pressure P_{56}, and a diffuser-exit static pressure P_{92}.

The restart control was implemented by means of a desk-top ±10-volt analog computer located in the wind tunnel control room. The computer was used to close loops between the feedback signals and the bypass door and centerbody servos. The logic which determined when the inlet was unstarted and which controlled the restart sequence was also programmed on the analog computer.

The restart control system was tested at Mach numbers of 2.50, 2.30, and 2.02, with the inlet coupled to the cold pipe. The control was also tested with the inlet coupled to a J85-13 engine at Mach numbers of 2.50 and 2.02 with the engine running at corrected speeds of 85 percent and 86.3 percent. respectively. In all tests, the inlet was unstarted by a reduction in inlet exit-corrected airflow. During the cold-pipe tests, the reduction in inlet-exit airflow was implemented by means of the bypass doors in two ways: (1) a pulse type closure of three symmetrically located bypass doors while the other three doors were used for control, or (2) addition of a pulse increase to the terminal shock control setpoint which caused a pulse type closure of the three control doors. When the inlet was

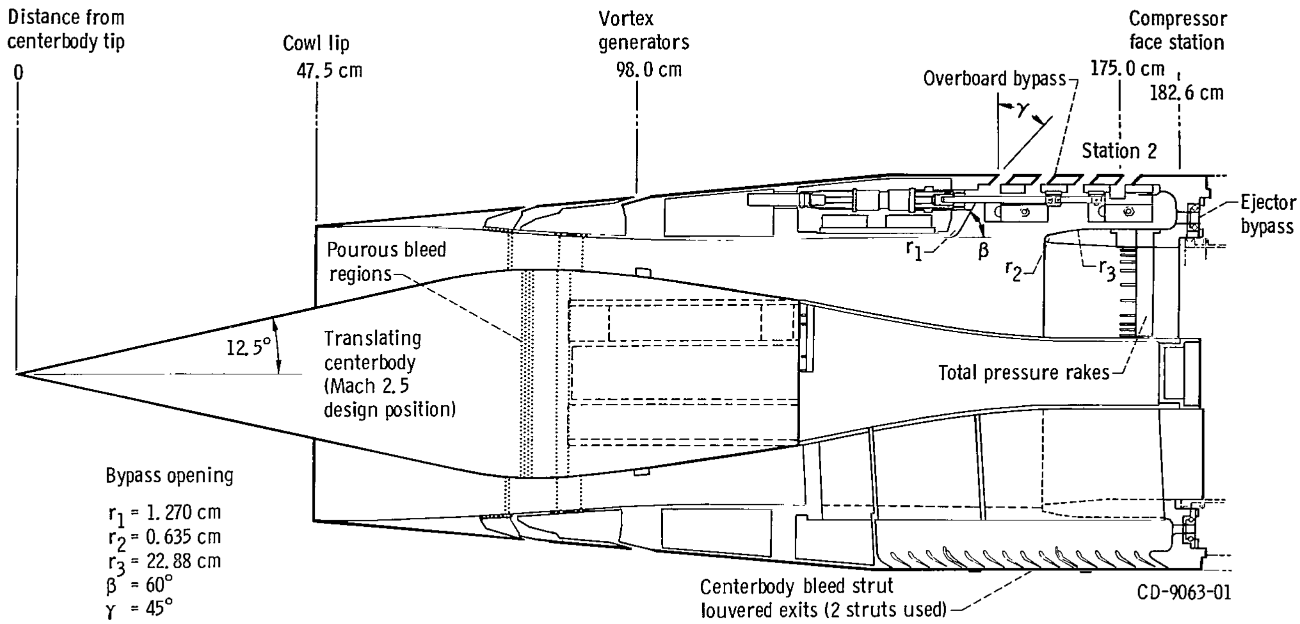

(a) Overall inlet details.

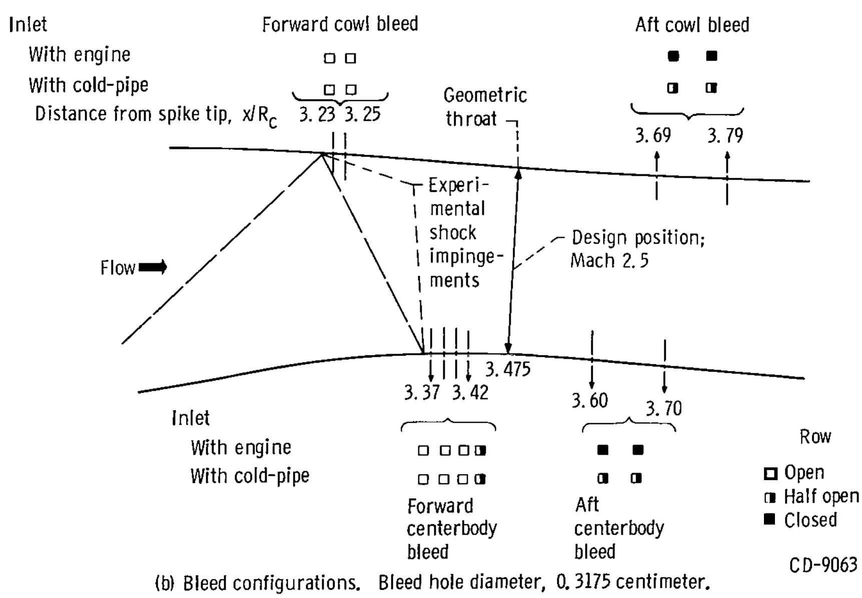

(b) Bleed configurations. Bleed hole diameter, 0.3175 centimeter.

Figure 2. - Inlet model details.

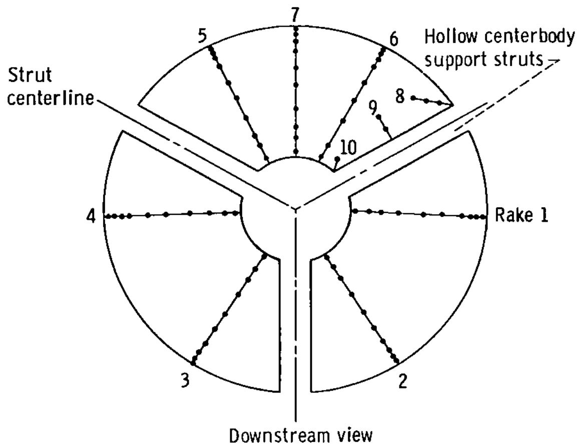

(c) Total-pressure instrumentation at diffuser station 2.

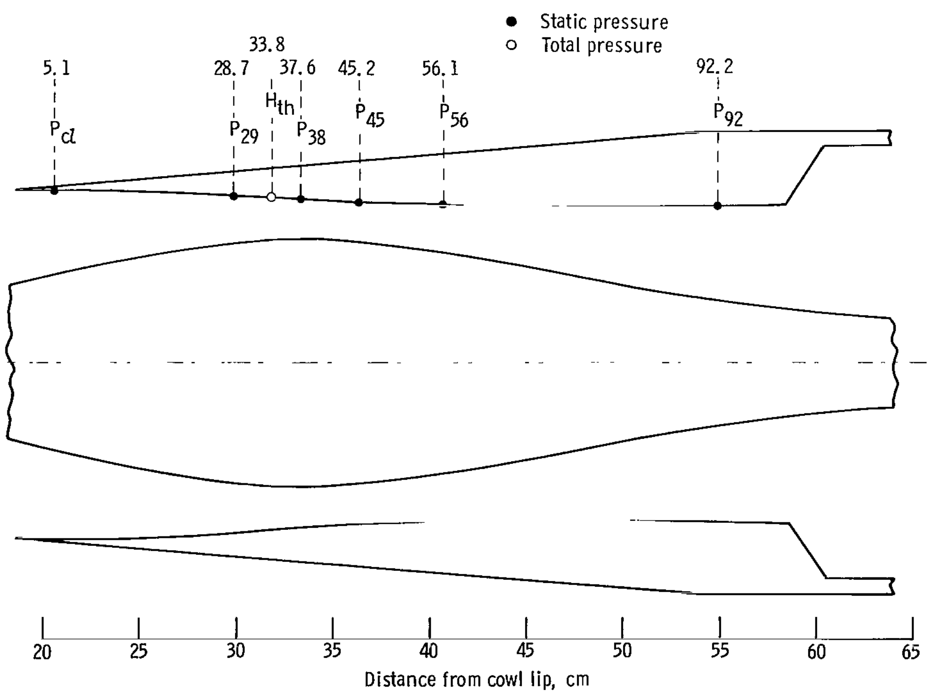

(d) Dynamic pressure transducer locations.

Figure 2. - Concluded.

coupled to the engine, a pulse increase was added to the setpoint which caused a pulse type closure of all six doors, since all six doors were used for control.

The restart controls were evaluated by monitoring the high-response pressure transducers in the inlet and the engine (when used) during the restart cycle. The multiple-probe rake instrumentation at the diffuser exit could only be used for determining steady-state pressure recovery and distortion. However, it was possible to infer inlet performance during controlled restart cycles by comparing values of P_{56} measured at steady-state peak recovery conditions and actual values of P_{56} during the restart cycle. During tests with the inlet coupled to the engine, the change in compressor discharge pressure ΔH_3 from the initial steady-state value H_3 was recorded. The transducer used to measure ΔH_3 was a quartz crystal type. The output of the transducer and its amplifier had the characteristics of a high-pass filter with a low-frequency corner at about 0.01 hertz and a high-frequency corner beyond 10 000 hertz. Bypass door position feedback voltage was also monitored during all restart tests. The control and disturbance bypass door traces that will be shown later are the sum of the control and disturbance bypass door position feedback voltages, respectively. The area variations between adjacent area notations on the ordinate of these traces are approximately linear.

RESTART CONTROL DESIGN BASIS

The following were selected as a design basis for the restart control: (1) Sense whether the inlet is started or unstarted, (2) change the inlet geometry to provide the required throat-to-capture area ratio for a restart when the inlet is unstarted, (3) return the inlet to the initial operating condition as quickly as possible, and (4) maintain high pressure recovery and low distortion by retaining terminal shock control throughout the restart cycle.

The restart control system was designed to accommodate downstream disturbances only. The restart control would have to be modified to accommodate an unstart due to upstream disturbances such as those caused by aircraft maneuvers and changes in atmospheric conditions. Modifications that might be required will be discussed in later sections.

TERMINAL SHOCK CONTROL

Inlet Steady-State Off-Design Pressure Recovery and Distortion

The steady-state loss in pressure recovery and increase in distortion that results from too large a bypass area can be illustrated by means of figures 3 and 4. These figures (taken from ref. 2) display experimental steady-state data with the inlet coupled to the cold pipe. For the cases shown, engine mass-flow actually refers to the choked-exit-plug mass flow.

Figure 3 shows typical internal cowl-surface static-pressure distributions for unstarted and started conditions. The curves are parametric with bypass door area. The sharp rises in static pressure indicate the position of the leading edge of a well defined terminal shock in the diffuser for both started and unstarted conditions. As expected the pressure profiles and the keys of figure 3 indicate that the terminal shock moves downstream (becomes more supercritical) as bypass area is increased, resulting in a loss of pressure recovery.

The performance map of figure 4 shows how steady-state total pressure recovery and airflow distortion at the compressor-face station vary with bypass area during a steady-

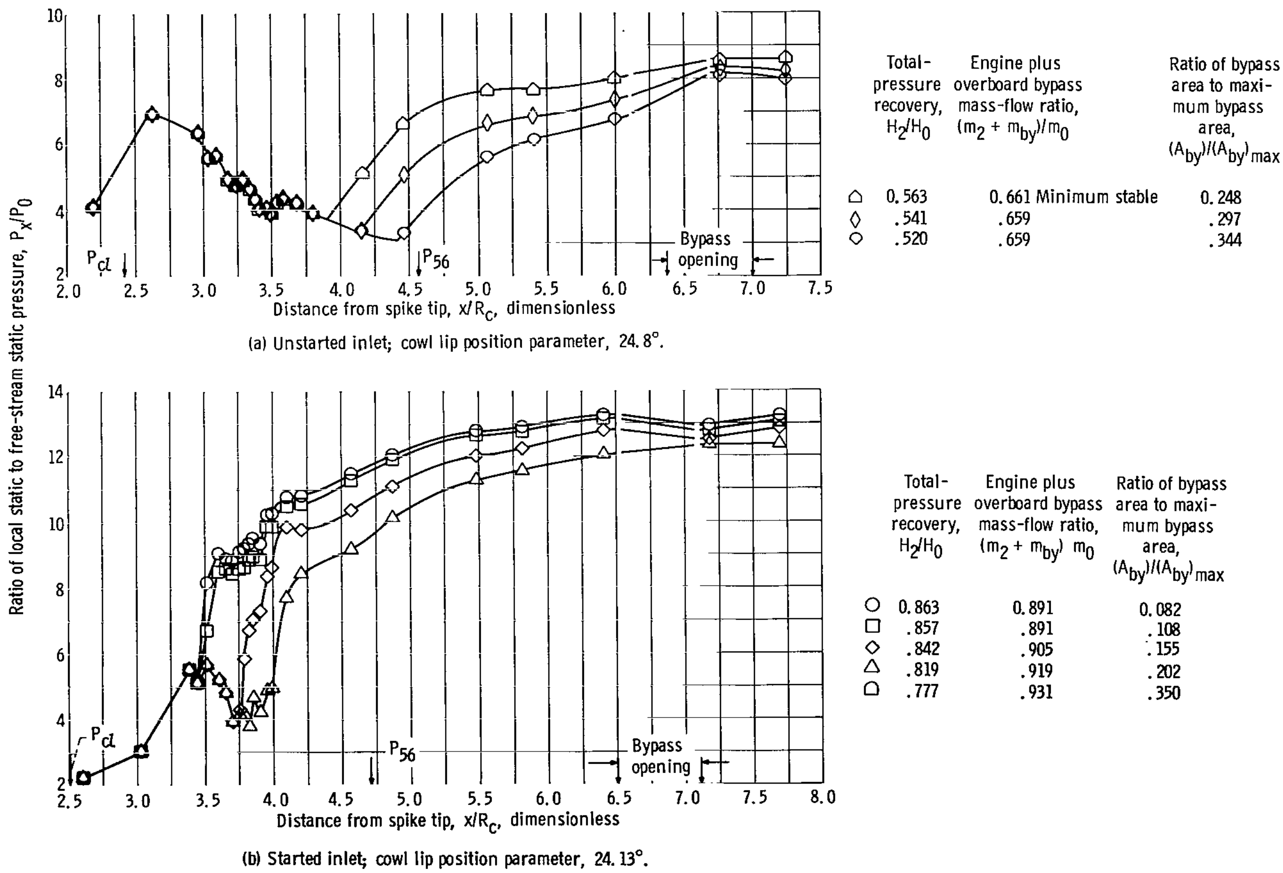

Figure 3. - Internal cowl-surface static-pressure distributions for various bypass area settings, fixed spike, and exit plug positions. Free-stream Mach number, 2.50; Reynolds number, 3.82×10^6; angle of attack, 0°; free-stream temperature, 317 K.

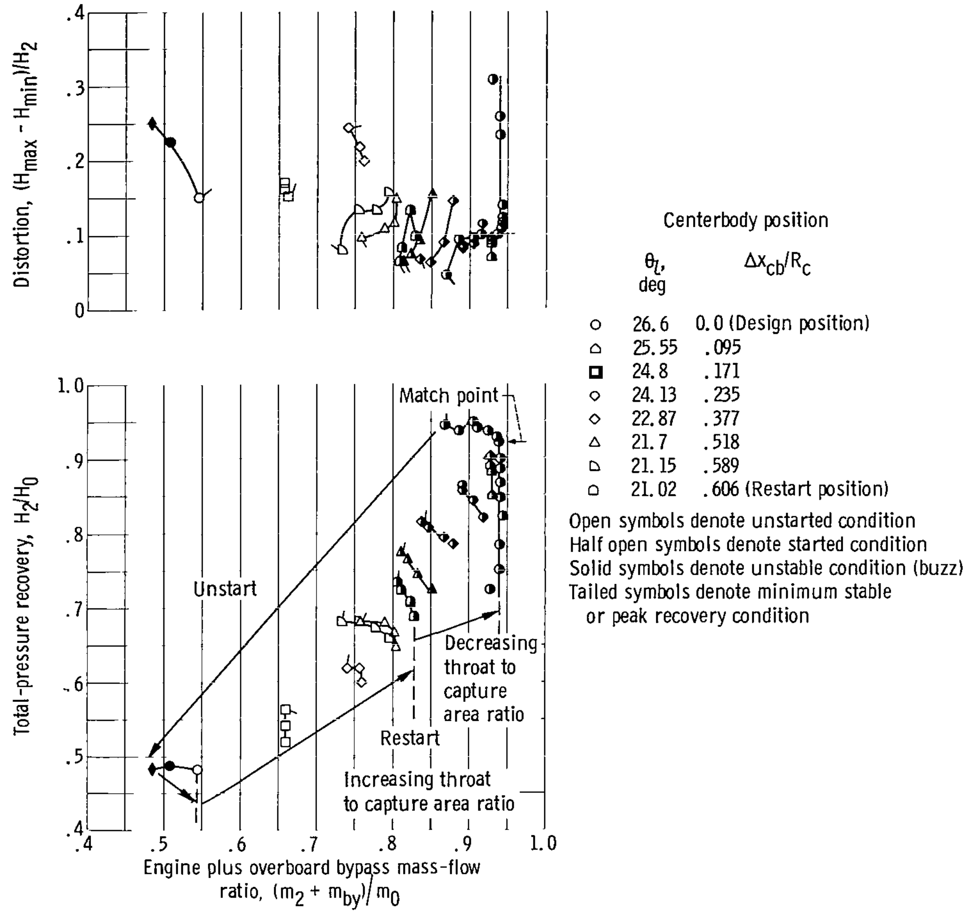

Figure 4. - Inlet total pressure recovery and distortion for various centerbody positions. Free-stream Mach number, 2.50; free-stream temperature, 317 K; Reynolds number, 3.82×10^6; ejector area to inlet capture area ratio, 0.0081; choked exit corrected airflow, 15.83 kilograms per second (except for ◑ at conditions other than match point).

state restart cycle at Mach 2.5. These curves are parametric with centerbody position. Figure 4 includes the pressure recovery and distortion data that correspond to the conditions for which static pressure distributions were shown in figure 3. The data shown for the other centerbody positions were also obtained by varying bypass door area, except when θ_l was 26.6° with the inlet started (◑ symbols). In that case, the bypass area was held constant and the choked plug was translated to vary terminal shock position thereby simulating an engine speed variation. The peak recovery and minimum distortion conditions (denoted by the tailed symbols) were achieved at the minimum allowable bypass area. A further reduction of bypass area resulted in an unstable-unstarted inlet condition. Increasing the bypass area generally increases distortion and decreases pressure recovery. The one exception occurred when θ_l was 22.87° with the inlet unstarted (◇ symbols). That condition is thought to be due to a flow separation region in the inlet (a further explanation is presented in ref. 2). Peak recovery conditions with the inlet started at θ_l's of 24.13° and 25.55° were not determined but are assumed to be close to the maximum values shown.

The arrows in figure 4 indicate the following successive inlet conditions: inlet unstart from the design centerbody position to a buzz condition, opening of the bypass doors to assure stable-unstarted inlet operation, extension of the centerbody with the inlet unstarted, and retraction of the centerbody with the inlet started. Figure 4 shows that, depending on how the bypass doors are manipulated during a restart cycle, total pressure recovery and distortion can vary over a wide range of values. The largest bypass area for the data shown in figure 4 was 35 percent of the fully open bypass area. No attempt was made to determine the maximum distortion and minimum pressure recovery that would result from larger bypass openings. As indicated earlier, the bypass doors were capable of passing 88 percent of the design inlet capture airflow. This value was chosen to accommodate the airflow reduction resulting from an engine stall. Thus, the possible increase in distortion and loss of pressure recovery is greater than that indicated by figure 4. However, by appropriate bypass door manipulation, it should be possible to achieve relatively high pressure recovery and low distortion during restart. A closed-loop terminal shock control would do a better job of maintaining high inlet pressure recovery and low distortion during a restart cycle than would scheduling of the bypass doors because of the unpredictable nature of engine airflow during such a transient. It was therefore decided to adapt one of the terminal shock controls that had been developed previously for this inlet (ref. 4) to function during the restart cycle.

Selection of Terminal Shock Control

In the previous terminal shock-control investigation (ref. 4), various types of high-response controllers using electronic compensation and multiple feedback loops had been evaluated. A block diagram of a system which was one of the best for control of terminal shock position in the presence of downstream airflow disturbances is illustrated in figure 5. The outer feedback loop senses throat-exit static pressure P_{56} as an indicator of terminal shock position. It is shown in reference 3 that P_{56} is a reliable indicator of actual terminal shock position. For sinusoidal airflow variations, the amplitude ratios of P_{56} and shock position agree within 0 to -3 decibels from 0 to 90 hertz. The error between actual P_{56} and $(P_{56})_{com}$ is transmitted to the bypass door servo through a proportional-plus-integral controller. A minor inner feedback loop using P_{92} provided more immediate sensing of engine-induced disturbances. A first-order high-pass filter in this loop eliminates low-frequency signals, thereby preventing low-frequency

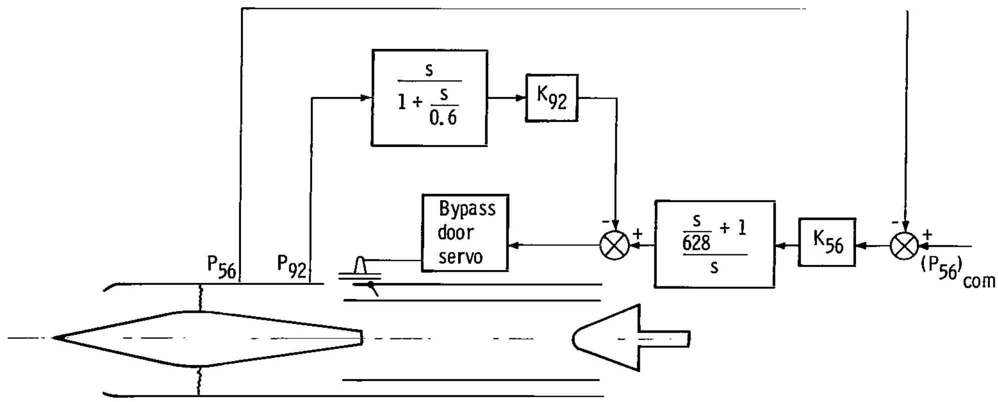

Figure 5. - Terminal shock controller with throat-exit (P_{56}) feedback and diffuser-exit (P_{92}) feedback.

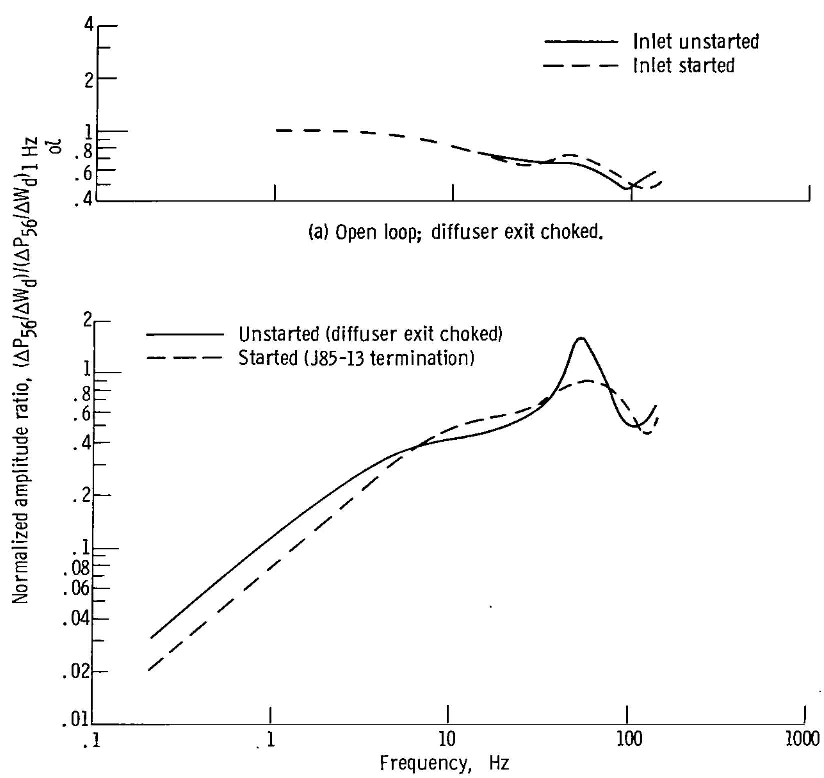

(b) Closed loop.

Figure 6. - Comparison of started and unstarted frequency responses of throat-exit static pressure to a sinusoidal downstream airflow disturbance without terminal shock control and with terminal shock control.

interaction of this loop which would cause improper setting of steady-state terminal shock position.

In order to design a closed-loop terminal shock control that would work during a restart cycle, it was necessary to determine the unstarted inlet dynamics. When the inlet is unstarted and the throat is choked, a secondary terminal shock exists. The started and unstarted open-loop frequency responses of P_{56} to a sinusoidal flow disturbance ΔW_d at the diffuser exit are displayed in figure 6(a). The ordinate is the ratio of the amplitude of the sinusoidal pressure perturbation ΔP_{56} divided by the amplitude of the sinusoidal flow disturbance ΔW_d. This ratio is, in turn, normalized by its value at 1 hertz. In the figure, it is noted that the frequency responses of P_{56} for the inlet in the started and unstarted conditions are not significantly different. Accordingly, closed-loop control of terminal shock position was tried with the inlet both started and unstarted using the control system of figure 5. The closed-loop frequency responses of the started and unstarted inlet are displayed in figure 6(b). The unstarted inlet is more resonant than the started inlet is at approximately 55 hertz. Although the inlet termination was not the same for both closed-loop tests of figure 6(b), the closed-loop response of the inlet was relatively unaffected by the termination (ref. 4). It was, therefore, concluded from figure 6(b) that the control of figure 5 could be used without modification to control both the started and unstarted inlet.

Terminal Shock Control Feedback Signal Setpoint Schedule

The throat-exit static pressure P_{56} was used as the terminal shock control feedback variable. During the previous terminal shock control investigation, it was found that a sign reversal occurs in the slope of the curve of P_{56} against shock position. A

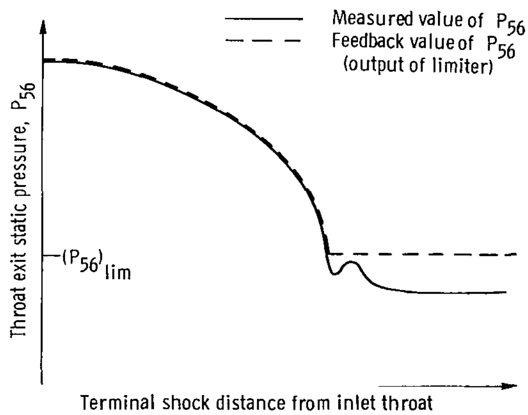

(a)

Figure 7. - Throat-exit static pressure P_{56} as function of terminal shock position.

sketch of the curve is shown in figure 7. This could have resulted in instability of the terminal shock control. Therefore, the feedback value of P_{56} was electronically limited (as shown by the dashed line in fig. 7) to prevent this. The throat-exit static pressure limit $(P_{56})_{lim}$ was set equal to 4.1 and 3.1 newtons per square centimeter (6 and 4.5 psia) during the cold pipe and engine tests, respectively. The difference was due to the change in the inlet bleed configuration that was made between the two test programs.

Figure 4 shows that, during a restart cycle, peak recovery increases as the centerbody is first extended and that it continues to increase after restart as the centerbody is retracted. The experimental peak values of P_{56} that correspond to the peak recovery conditions of figure 4 are tabulated as a function of dimensionless centerbody position in table I. The data show that in order to maintain the highest possible recovery during a restart cycle, it is necessary to schedule the terminal shock control setpoint or command $(P_{56})_{com}$ as a function of centerbody position. Two schedules were used: one for the started inlet and one for the unstarted inlet. The $(P_{56})_{com}$ schedules were programmed on the analog computer as either continuous or stepwise continuous functions of centerbody position. Relay comparators on the analog computer were used to implement the step schedules. The continuous schedules consisted of straight line segments and were im-

TABLE I. - VALUES OF P_{56}/P_0 (CORRESPONDING TO PEAK CONDITIONS OF FIG. 4) AS A FUNCTION OF CENTERBODY POSITION,

[Free-stream static pressure, 0.53 N/cm^2 (0.77 psi).]

Centerbody position, $\Delta x_{cb}/R_c$	Pressure ratio, P_{56}/P_0	
	Unstarted	Started
0	4.45	12.81
.095	----	[a]11.40
.171	5.13	-----
.235	----	[a]11.44
.377	7.22	11.34
.518	9.00	10.43
.589	9.29	-----
.606	----	9.09

[a]Near-peak values.

plemented by means of diode function generators. During tests of the restart control system with the inlet coupled to the cold pipe, the $(P_{56})_{com}$ schedules were determined experimentally. Two stepwise continuous schedules and one continuous schedule, which were determined experimentally for the case where $M_0 = 2.50$, are shown in figure 8. The schedules were determined in the following manner. Initially, the $(P_{56})_{com}$ level on each step was set at a low value by adjusting a potentiometer for each on the analog computer. A series of restart cycles was then run. Before each successive restart of the series, the $(P_{56})_{com}$ level for the same step was adjusted upward by 0.34 newton per square centimeter (0.5 psi). This procedure was repeated until the inlet went into buzz during the unstarted part of the cycle or unstarted again during the started part of the cycle. The final $(P_{56})_{com}$ level scheduled for each step was the highest value that had resulted in a successful restart. The segments of the continuous schedules were established in essentially the same manner.

It can be seen in figure 8, that the dynamic experimental method used to determine the $(P_{56})_{com}$ schedules occasionally resulted in $(P_{56})_{com}$ levels being scheduled that were slightly higher than the corresponding steady-state peak values of P_{56}. Ordinarily, it might be assumed that this would unstart the inlet. However, after a step change in $(P_{56})_{com}$, up to 40 milliseconds was required for P_{56} to reach $(P_{56})_{com}$. By this time, the spike had reached a position that permitted higher values of P_{56}. In other instances $(P_{56})_{com}$ was below $(P_{56})_{lim}$. In these cases, the negative error signal to the terminal shock controller held the bypass doors open resulting in lower values of P_{56} than $(P_{56})_{com}$

For a flight application, the more conservative steady-state terminal shock control command values should be used rather than those obtained by the trial and error technique. This should be possible to do without a large penalty in recovery. Such a procedure was applied during this program in the case of the inlet terminated by the J85-13 engine. The continuous schedule of $(P_{56})_{com}$ shown in figure 8 for the inlet with cold pipe offers the advantage of permitting higher $(P_{56})_{com}$ values than does the step schedule without exceeding the peak steady-state values. In addition, this type of schedule results in smoother operation of the bypass doors. Despite the advantages of the continuous schedule, the step-type schedules were used more frequently during the restart control test program because of convenience of implementation and making changes for different wind tunnel conditions.

In general, different $(P_{56})_{com}$ schedules might be required for different Mach numbers, angles-of-attack, and other possible disturbances in flight conditions.

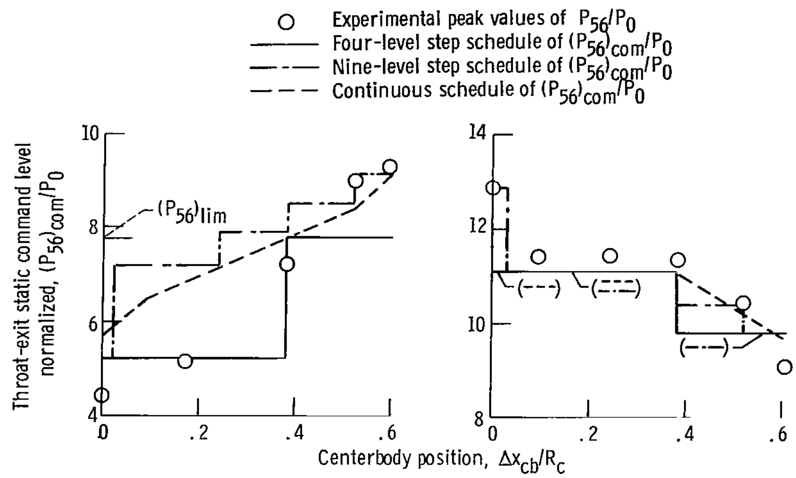

(a) Unstarted $(P_{56})_{com}$ schedules. (b) Started $(P_{56})_{com}$ schedules.

Figure 8. - Peak values of ratio of throat-exit static pressure to free-stream static pressure (P_{56}/P_0) corresponding to peak recovery condition of figure 4 and $(P_{56})_{com}/P_0$ schedules as functions of centerbody position. Free-stream Mach number, 2.50; free-stream static pressure, 0.53 newton per square centimeter (0.77 psi).

UNSTART CONTROL SIGNAL

The ratio of a static pressure just aft of the cowl lip P_{cl} to a throat total pressure H_{th} was used to indicate when the inlet was unstarted. When an unstart occurs, the cowl-lip static pressure increases because of the transition from supersonic to subsonic flow. (The difference between P_{cl} for started and unstarted conditions at approximately the same centerbody position can be seen in fig. 3.) At the same time, the throat total pressure decreases because of the large recovery loss associated with an unstart. (The difference in recovery H_2/H_0 for started and unstarted conditions is also indicated in the keys in fig. 3.) Thus, the ratio P_{cl}/H_{th} is low for started conditions and high for unstarted conditions.

A started or unstarted inlet was indicated by comparing the measured ratio to a reference value and noting whether the measured value was lower (started condition) or higher (unstarted condition) than the reference value. Traces of measured values of

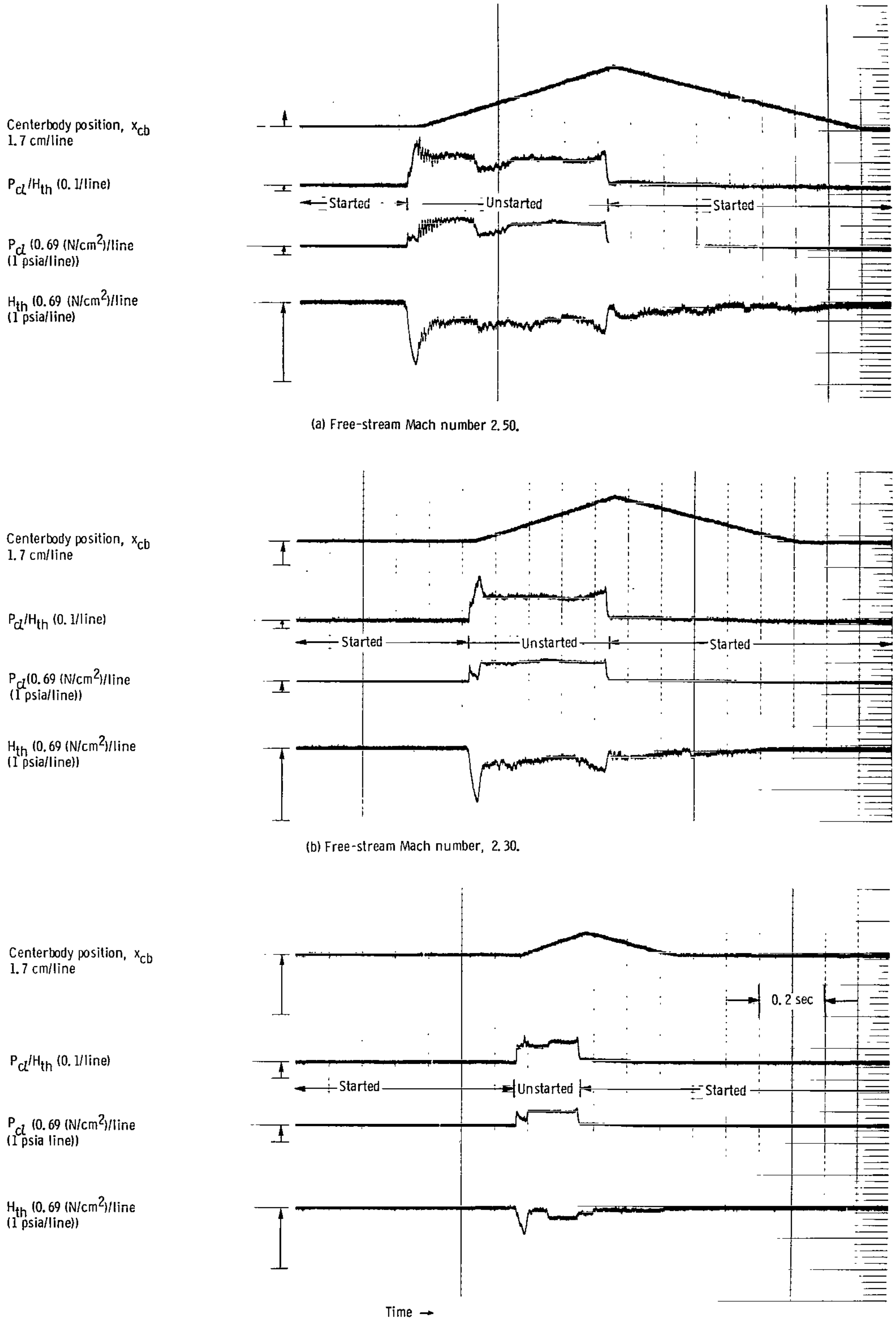

(a) Free-stream Mach number 2.50.

(b) Free-stream Mach number, 2.30.

(c) Free-stream Mach number, 2.02.

Figure 9. - Measured values of centerbody position (x_{cb}), cowl-lip static pressure (P_{cl}), throat total pressure (H_{th}), and ratio of cowl-lip static to throat total pressure as functions of time and free-stream Mach number for started and unstarted conditions. Free-stream total temperature, 317 K; Reynolds number, 3.8×10^6; ratio of ejector bypass area to inlet capture area, 0.0109; choked-exit plug corrected airflow, 14.3 kilograms per second.

P_{cl}, H_{th}, P_{cl}/H_{th}, and centerbody position as functions of time for both the started and unstarted inlet are shown in figure 9 for Mach numbers of 2.50, 2.30, and 2.02. In the figures, the arrows indicate the direction of increasing magnitude, and the bases of the arrows are at zero magnitude. The centerbody position trace represents translation from the fully retracted position. This was slightly aft of the Mach 2.50 design centerbody position. In order to use the same values of $(P_{cl}/H_{th})_{ref}$ for the range of Mach numbers 2.02 to 2.50, it is necessary that the lowest unstarted value of P_{cl}/H_{th} be higher than the highest started value at any of those Mach numbers. In this inlet this was not possible because the lowest unstarted value of P_{cl}/H_{th} at Mach 2.50 was not higher than the highest started value of P_{cl}/H_{th} at Mach 2.02, both having a value of approximately 0.3. This problem was accommodated in the inlet restart control by manual adjustment of $(P_{cl}/H_{th})_{ref}$. A value of 0.275 was used for Mach 2.50 and 2.30 while 0.350 was used for Mach 2.02. For a flight application, this setpoint could be scheduled in a simple fashion as a function of inlet Mach number.

RESTART CONTRACTION RATIO

After the inlet unstarted, it could only be restarted by increasing the ratio of throat area to cowl-lip flow area. This was done by translating the centerbody forward, which increased throat area while decreasing the cowl-lip flow area. Since the design basis of the restart control system called for restarting the inlet as quickly as possible, the centerbody was slewed at its maximum rate. The restart control always returned the centerbody to its initial started position. This works satisfactorily for the case of a downstream unstart disturbance. However, for some types of upstream unstart disturbances, a centerbody control might be required to assure an inlet restart.

COMPLETE RESTART CONTROL SYSTEM

A diagram of the complete inlet restart control system is given in figure 10. The measured ratio P_{cl}/H_{th} was continuously compared with a reference value. When an unstart was indicated the following restart cycle was initiated:

(1) The centerbody was commanded to translate forward at its maximum slewing rate to increase throat-to-capture area ratio.

(2) At the same time, the unstarted $(P_{56})_{com}$ schedule was switched in. The terminal shock control continuously adjusted the bypass doors to eliminate the error in P_{56}.

(3) When the inlet restarted, the measured value of P_{cl}/H_{th} dropped below $(P_{cl}/H_{th})_{ref}$.

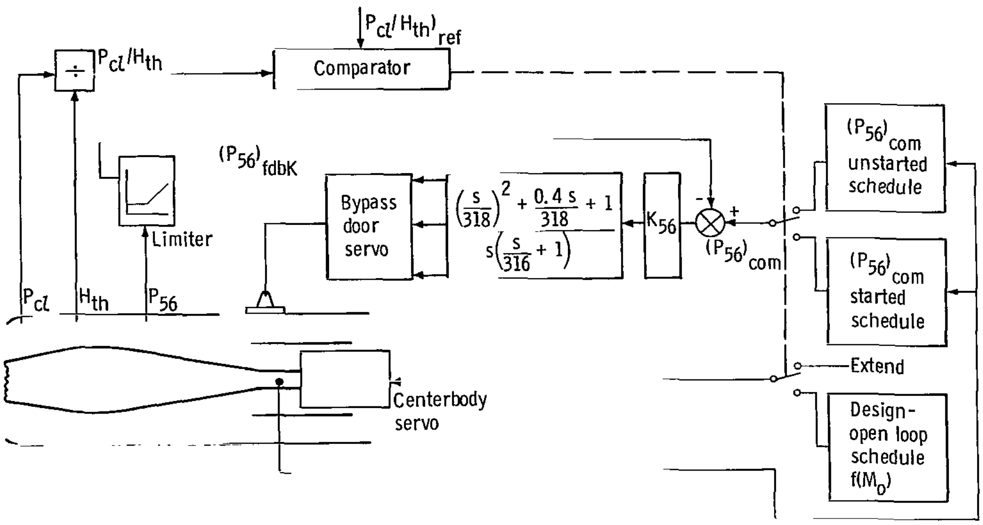

Figure 10. - Restart control system.

(4) When restart was indicated, $(P_{56})_{com}$ was switched back to the started schedule, and the centerbody was retracted to its initial position. At the completion of the restart cycle, the inlet was at its initial started condition.

The terminal shock control actually used in the inlet restart work utilized a single feedback loop for control of shock position. This is contrasted with the two-loop terminal shock control shown in figure 5, which gave the closed-loop frequency responses of figure 6(b). The change was made because, although the two-loop control gave good results for sinusoidal disturbances in inlet weight flow with the inlet either started or unstarted, the inner loop created a problem when the inlet experienced the large transient of unstarting. When the inlet unstarted, the sharp drop in P_{92} caused the inner loop to supply a signal which initially drove the bypass doors in the closed direction. The simultaneous drop in P_{56} results in an outer loop error signal which also drives the bypass doors in the closed direction until $(P_{56})_{com}$ is switched to the low levels of the unstarted schedule. However, when the inlet unstarts, the bypass doors must be opened in order to choke the throat which suppresses buzz. The P_{92} feedback was eliminated to reduce the undesired closure of the bypass doors. It is possible that, with further development, the inner P_{92} loop could either be maintained continuously or simply switched out during part or all of the restart cycle. The delay in switching to the unstarted $(P_{56})_{com}$ schedule (about 0.01 sec) was due to the switching time of the relay comparator used in the unstart signal circuit. Using an electronic comparator could reduce, if not eliminate, the undesirable bypass door closure due to the outer P_{56} loop.

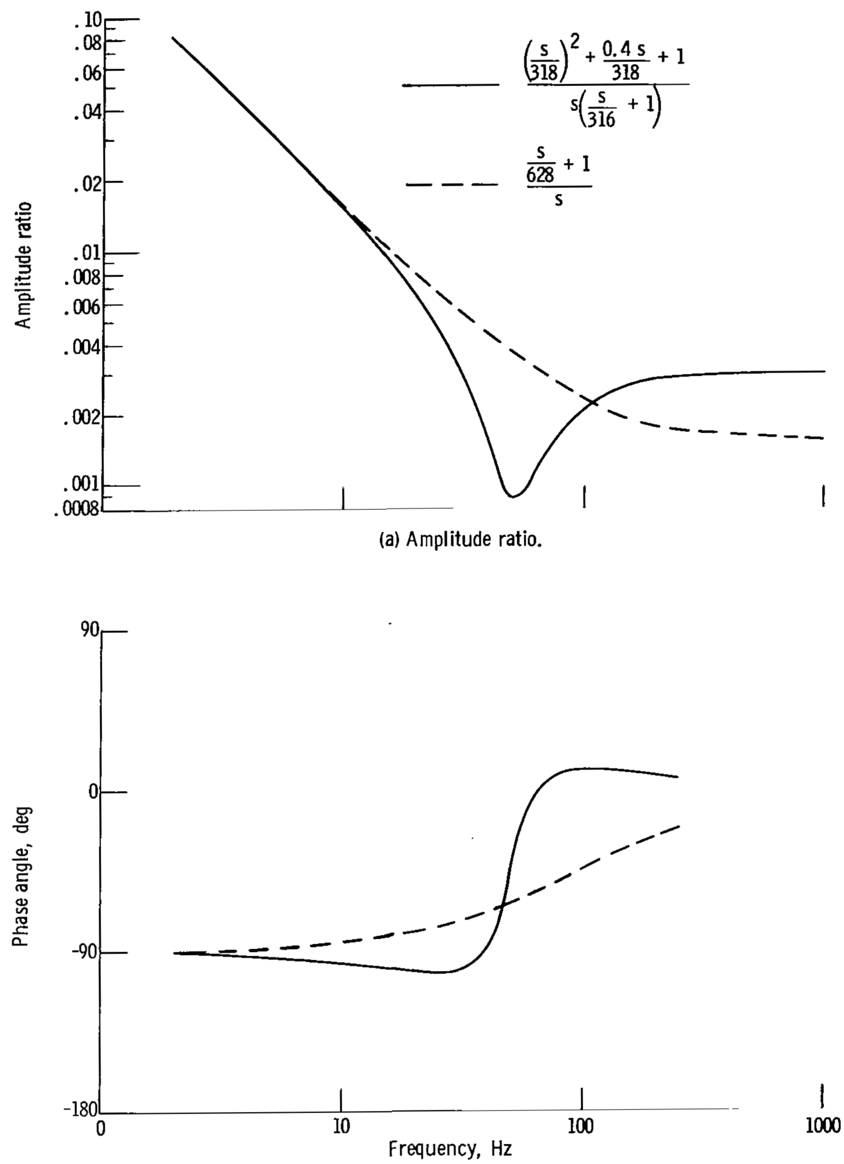

(a) Amplitude ratio.

(b) Phase angle.

Figure 11. - Comparison of amplitude and phase characteristics of two terminal shock controllers.

A change in the forward path controller transfer function is also noted between figures 5 and 10. The controller transfer function of figure 10 is a refinement of the proportional-plus-integral control of figure 5. It was used in the later work with the terminal shock control. The amplitude and phase characteristics of the two terminal shock controllers are displayed in figure 11. The more complicated transfer function behaves like a simple proportional-plus-integral controller except in the region of the corner frequency of about 318 radians per second (50.5 Hz). Here, it has a lower amplitude ratio than the simple controller. This lower amplitude characteristic of the more complex controller was of benefit in controlling terminal shock position because the uncontrolled inlet had a resonance at about 50 hertz (see fig. 6(a)).

RESULTS AND DISCUSSION

Cold-Pipe Tests

The restart control was first tested with the inlet coupled to the cold pipe at a free-stream Mach number of 2.50. Results of tests using the three different $(P_{56})_{com}$ schedules of figure 8 are shown in figure 12. In figure 12, the centerbody position trace represents centerbody translation from the fully retracted position. The arrows in the figure indicate the direction of increasing magnitude of the variables and the base of each arrow is at zero magnitude.

The following is a description of the major events that occurred during the restart cycle at Mach 2.50 shown in figure 12(a) (the numbers correspond to the same numbers in the figure):

(1) The terminal shock was initially placed on the verge of unstart (between the P_{29} and P_{38} locations).

(2) A pulse decrease in disturbance door area caused the terminal shock to move upstream, as indicated by the increase in inlet pressures.

(3) The initial increase in P_{56} is sensed by the terminal shock control. Since it indicates a forward moving shock position, the bypass doors were commanded to open to restore shock position to prevent inlet unstart.

(4) Despite the terminal shock control action, a net decrease in bypass weight flow was created. The inlet unstarted and the throat static pressures dropped abruptly. The yet intact terminal shock controller interpreted the drop in P_{56} as being due to an aft shock motion. It commanded the bypass doors to close (which is the opposite direction desired) to raise inlet pressure recovery.

(5) The unstart signal exceeded the reference value of 0.275.

(6) After a delay of approximately 0.01 second, the terminal shock control command signal $(P_{56})_{com}$ was switched to the unstarted schedule. The delay was due to the mechanical relay comparator used in the unstart signal circuit.

(7) $(P_{56})_{com}$ was set at 2.8 newtons per square centimeter (4 psia) after the comparator switched. Since this was lower than the limit value of P_{56} of 4.1 newtons per square centimeter (6 psia), a negative error signal commanded the bypass doors full open. This resulted in choking of the throat which eliminated buzz. Although some

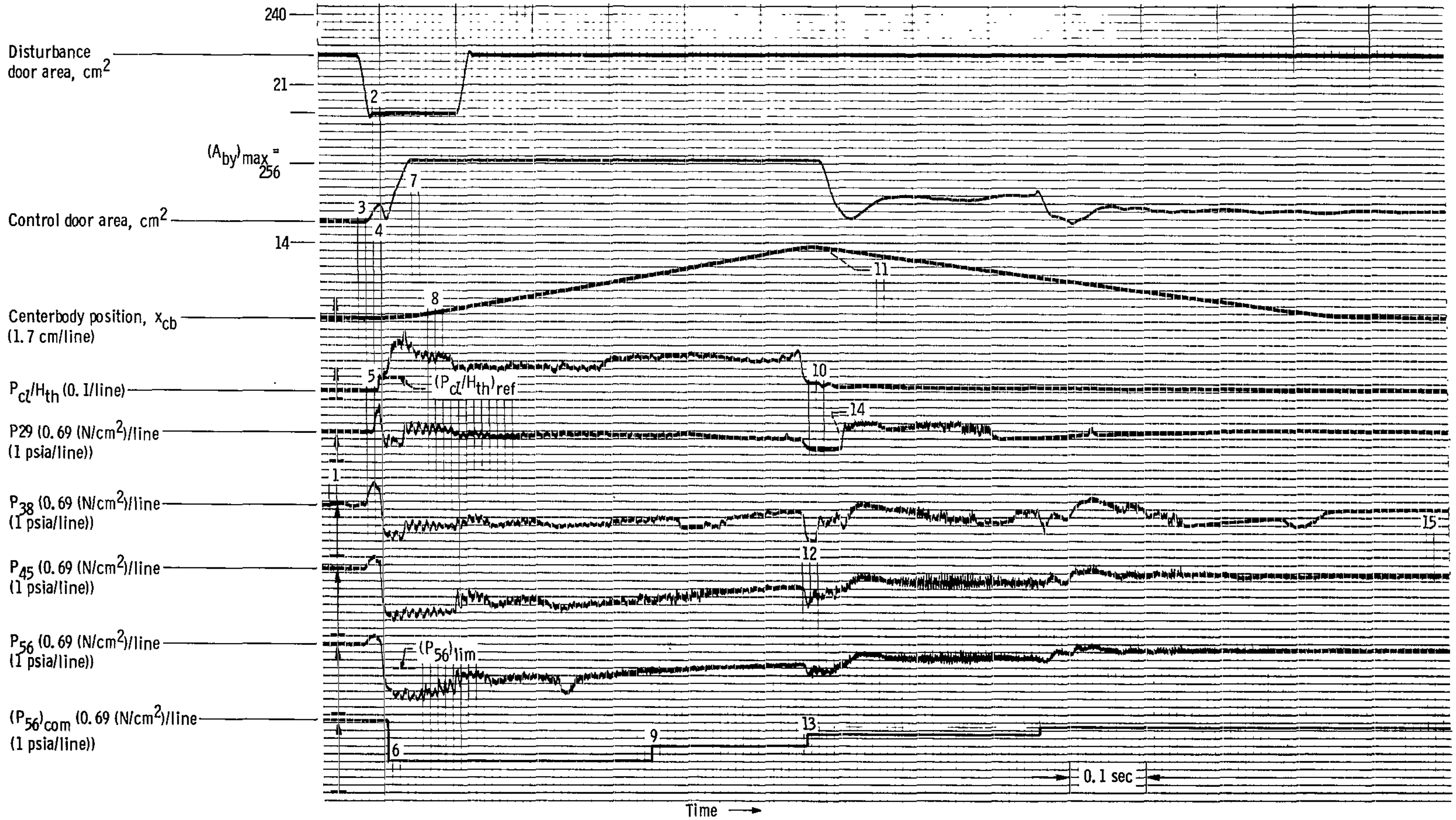

(a) Four-level $(P_{56})_{com}$ step schedule.

Figure 12. - Inlet unstart followed by controlled restart using various command throat-exit static pressure ($(P_{56})_{com}$) schedules. Free-stream Mach number, 2.50; free-stream temperature, 317 K; Reynolds number, 3.8×10^6; ratio of ejector bypass area to inlet capture area, 0.0103; choked-exit plug corrected airflow, 14.3 kilograms per second.

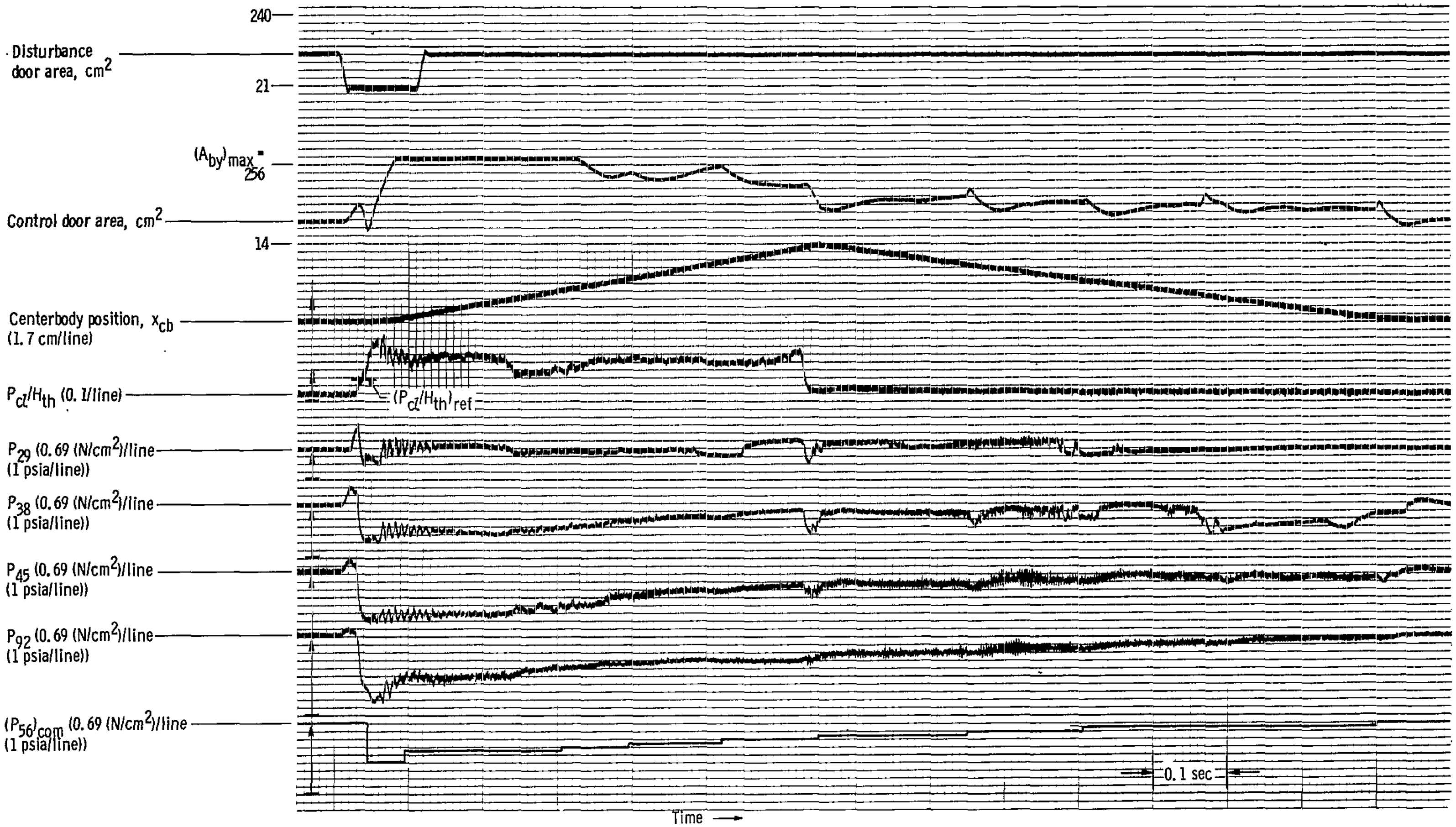

(b) Nine-level $(P_{56})_{com}$ step schedule.

Figure 12. - Continued.

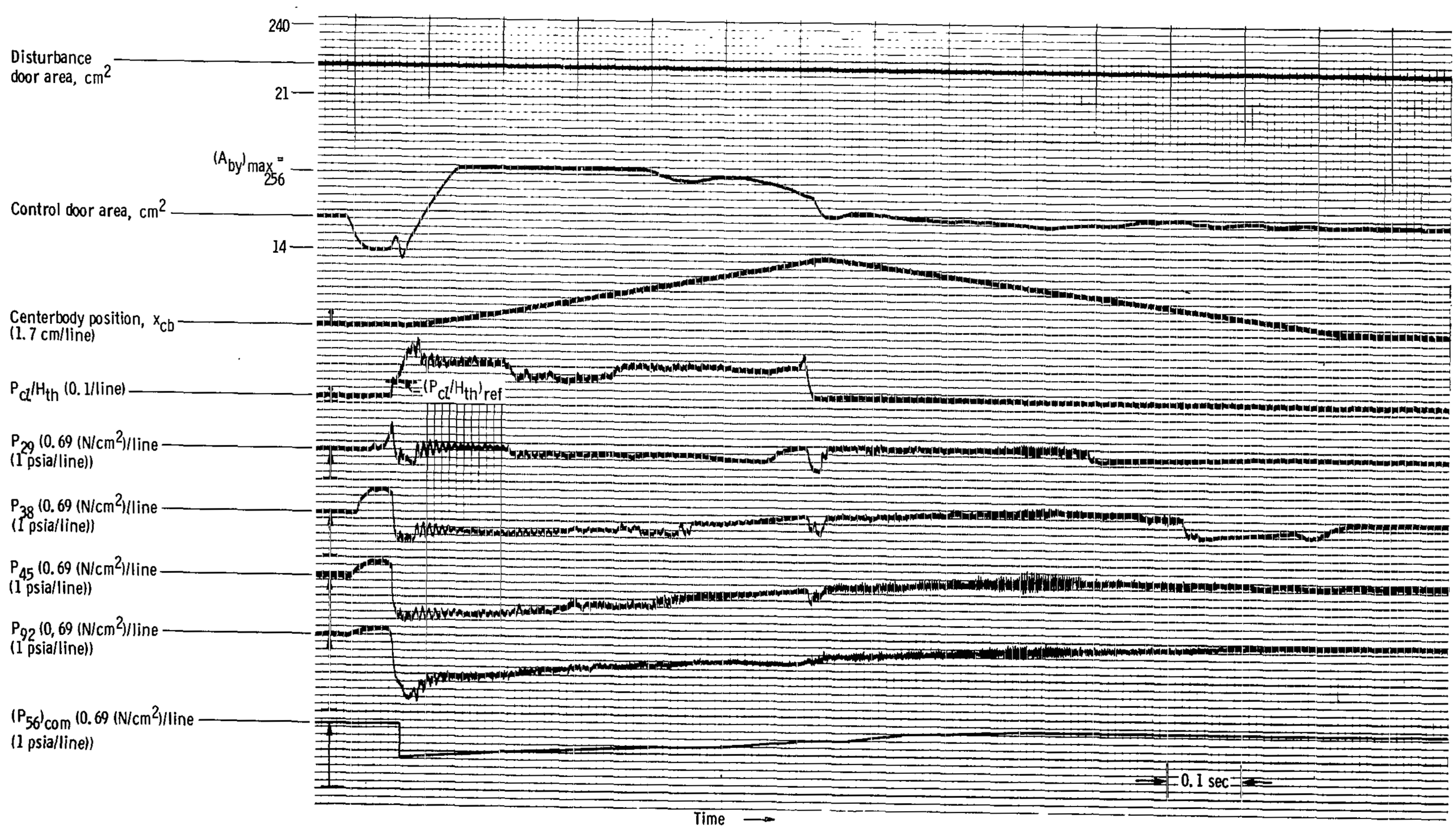

(c) Continuous $(P_{56})_{com}$ schedule.

Figure 12. - Concluded.

oscillations in the inlet pressure traces did exist for approximately 0.1 second after unstart occurred, they are not of sufficient magnitude to constitute a buzz condition.

(8) The indication of an unstart also signaled the centerbody to extend.

(9) $(P_{56})_{com}$ was stepped down to a value of approximately 4.1 newtons per square centimeter (6 psia), the same value as $(P_{56})_{lim}$. The $(P_{56})_{com}$ levels were set by means of potentiometers on the analog computer. Since the bypass doors remained at the fully open position, a negative error still existed $\left((P_{56})_{com} < (P_{56})_{lim}\right)$.

(10) Restart was indicated by the unstart signal dropping below the reference value.

(11) The centerbody travel was reversed after a delay of approximately 0.02 second and started to slew at maximum velocity in the aft direction.

(12) The restart transient indicates that the terminal shock first moved to a position between P_{38} and P_{45}. Notice that P_{38} dropped and remained at a low constant level which is indicative of supersonic flow. The P_{45} trace does not indicate supersonic flow. The shock subsequently moved upstream of P_{38} as indicated by the sharp increase in P_{38}.

(13) When restart was sensed, the terminal shock controller switched to the started $(P_{56})_{com}$ schedule. The $(P_{56})_{com}$ was then higher than the limited $(P_{56})_{fdbk}$ resulting in a positive error signal to the shock position controller. This commanded the control doors to close. As P_{56} responded by increasing above the commanded value, typical hunting action of a closed-loop control took place.

(14) The initial decrease in control door area resulted in moving the shock to a position upstream of P_{29}. A corresponding increase occurred in the other inlet pressures.

(15) The combination of centerbody retraction and bypass door control resulted in the terminal shock returning to a position between P_{38} and P_{45}. The terminal shock control maintained P_{56} close to the commanded level throughout the started portion of the cycle.

The restart control test displayed in figure 12(b) utilized a nine-level schedule of $(P_{56})_{com}$ as contrasted with the four-level schedule of the test of figure 12(a). In the test displayed in figure 12(c), a continuous schedule of $(P_{56})_{com}$ was used. The levels of $(P_{56})_{com}$ scheduled for the cases shown in figures 12(b) and (c) were generally higher than those scheduled for the case shown in figure 12(a). Therefore, better performance was achieved during the restart cycles of figures 12(b) and (c). It can be seen that the bypass doors moved from the fully open position before the inlet restarted for the restart cycles of figures 12(b) and (c). It can also be seen that the terminal shock moved to a more supercritical position during the restart transients of figure 12(a) than it did during the restart transients of figures 12(b) and (c). This fact can be observed from the trace of P_{38} which exhibits the largest dip during the restart transient of figure 12(a). The less supercritical shock excursion results in a lower level of distortion which is particularly desirable if an engine is operating at the time the restart transient occurs.

A continuous schedule of the type shown in figure 12(c) is concluded to be better than a step schedule because (1) it allows generally higher levels of $(P_{56})_{com}$ to be scheduled which results in lower distortion and higher pressure recovery, (2) inlet pressure variations are smoother which is desirable when an engine is running, and (3) bypass door positioning is smoother (a hardware advantage).

The complete restart cycle for the three schedules illustrated in figure 12 took approximately 1.4 seconds. This time was limited by the maximum slewing rate of the centerbody. The maximum slewing rate was governed by the design of the centerbody hardware.

In order to demonstrate that the restart control system would operate at other free-stream Mach numbers, tests were conducted at Mach 2.30 and 2.02. The results of these tests are shown in figure 13. Stepwise continuous $(P_{56})_{com}$ schedules were used in both tests. Somewhat lower pressures had to be scheduled at Mach 2.30 and 2.02 because the wind tunnel total pressure was lower for those conditions than for the Mach 2.50 condition. The same general sequence of events that was described for the restart cycle shown in figure 12(a) also occurred during the tests shown in figure 13. Some of the differences between the restart cycles at Mach 2.50 and those at Mach 2.30 and 2.02 will be discussed in the following paragraphs.

For the Mach 2.30 case (fig. 13(a)), the centerbody was positioned approximately 6.3 centimeters ahead of the Mach 2.50 design position to give the required throat area for Mach 2.30 operation. Since restart time depended on centerbody slewing velocity and net centerbody translation, a reduction of cycle time from 1.4 seconds at Mach 2.5 to 1.0 second at Mach 2.30 resulted.

For the Mach 2.02 case (fig. 13(b)), it was necessary to increase the value of $(P_{cl}/H_{th})_{ref}$ from 0.275 (used for both Mach 2.50 and 2.30 cases) to 0.350. The centerbody had to be positioned approximately 15.7 centimeters ahead of the Mach 2.50 design position to give the required throat area for Mach 2.02 operation. The net centerbody translation required to restart the inlet was less at Mach 2.02 than at either Mach 2.50 or 2.30. The restart cycle time was thus reduced to approximately 0.5 second at Mach 2.02. Comparison of the P_{92} traces in figures 12(c) and 13(a) and (b) indicate that the unstart transient at Mach 2.02 was milder than those at Mach 2.50 or 2.30. This can also be seen by comparing steady-state data from reference 2 which shows that the ratio of total pressure recovery just after unstart to that just before unstart is approximately 0.51, 0.69, 0.89 for Mach 2.50, 2.30, and 2.02, respectively. Results of the engine tests, to be shown later, indicate that the severity of the unstart transient has a considerable effect on engine operation.

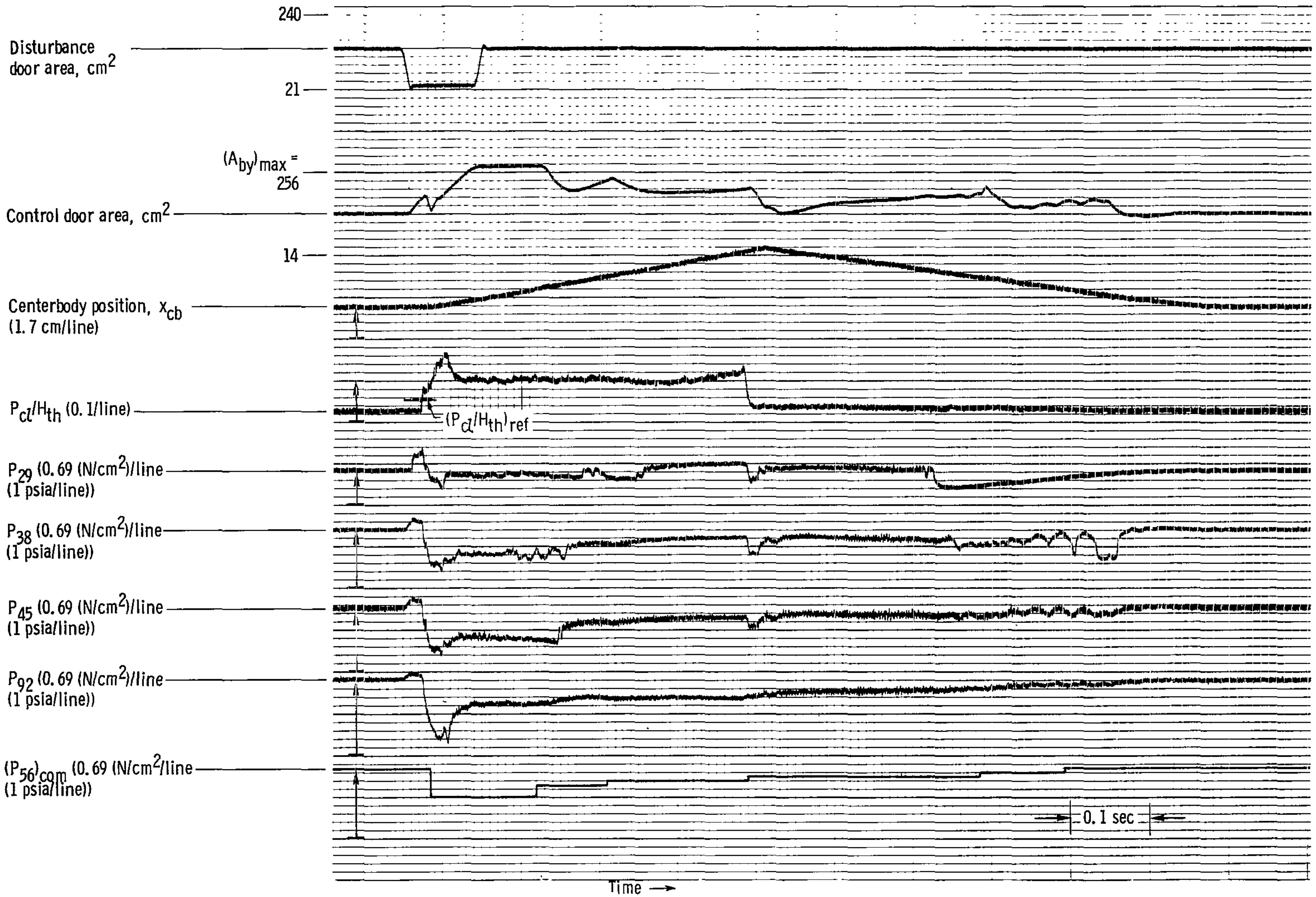

(a) Free-stream Mach number, 2.30.

Figure 13. - Inlet unstart followed by controlled restart at off-design free-stream Mach numbers. Free-stream temperature, 317 K; Reynolds number, 3.8×10^6; ratio of ejector bypass area to inlet capture area, 0.0109; choked-exit plug corrected airflow, 14.3 kilograms per second.

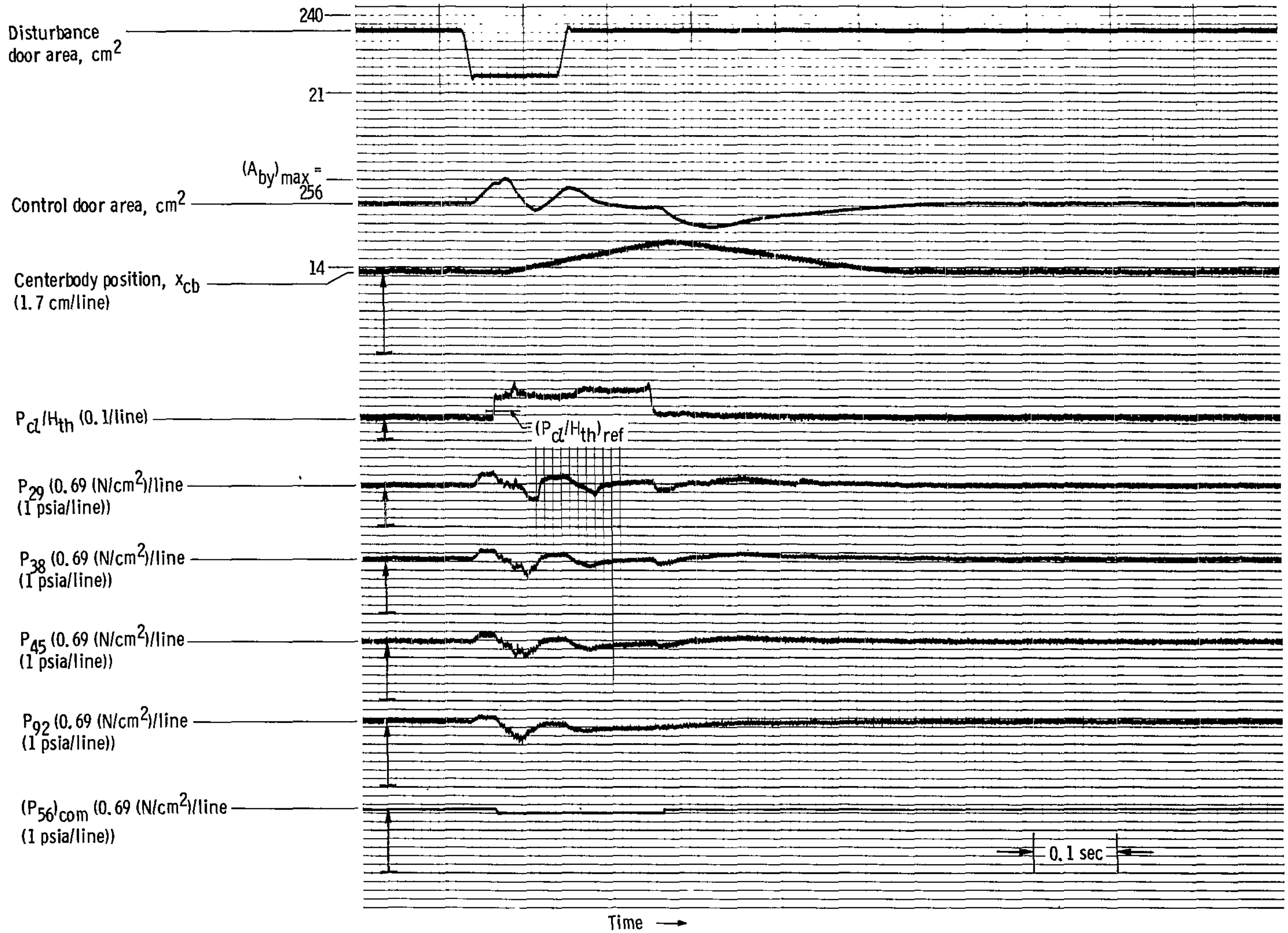

(b) Free-stream Mach number, 2.02.

Figure 13. - Concluded.

Engine Tests

The restart control system was also tested with the inlet coupled to a J85-13 turbojet engine. The major objectives of these tests were to (1) determine whether the engine would operate normally during the restart cycle, and (2) to see whether the restart control would work properly if compressor stall occurred at any time during the unstart - restart transient.

Results of restart control tests at Mach 2.02 and 2.50 are shown in figures 14 and 15, respectively. The restart control was first tested with the engine at a free-stream Mach number of 2.02 because of the mildness of the unstart transient at Mach 2.02. Three tests at Mach 2.02 are shown in figure 14. In each case, the corrected engine speed was the same (86.3 percent) but the initial total pressure ratio across the compressor H_3/H_2 was different. A five-level $(P_{56})_{com}$ step schedule was used in all three cases. An unstart followed by a controlled restart where the initial H_3/H_2 value was 4.16 is shown in figure 14(a). The normal operating line value of H_3/H_2 for a corrected speed of 86.3 percent is approximately 4.40. The inlet was unstarted by pulsing the six control doors simultaneously. As noted in figure 14(a), the engine mechanical speed and exhaust gas temperature traces held constant. It thus appears that the engine continued to operate normally throughout the restart cycle. As expected the restart control returned the inlet to the initial operating condition in the same time that was required with the cold-pipe termination (approx. 0.5 sec). There did not seem to be any major difference between this restart cycle and the one at Mach 2.02 with the inlet coupled to the cold pipe (fig. 13(b)).

Figure 14(b) shows a controlled restart at Mach 2.02 where the initial value of H_3/H_2 was 4.52. In this case ΔH_3 experienced a sudden decrease of approximately 22 newtons per square centimeter (32 psia) from its initial value of approximately 28 newtons per square centimeter (40 psia). Simultaneously, H_2 dips to a value of approximately 2.1 newtons per square centimeter (3 psia), then recovers to approximately 5.5 newtons per square centimeter (8 psia). Thus, the initial H_3/H_2 of 4.52 decreased to a minimum of approximately 2.6 but within 0.1 second after the unstart H_3/H_2 returned to approximately 4.5. Closer inspection of the H_2 trace discloses a sharp spike in pressure approximately 0.02 second after the inlet unstart. Similar spikes of pressure are noted in the P_{56} and P_{29} traces. This characteristic is thought to be indicative of the occurrence of a hammer shock in the inlet caused by a sudden reduction in engine airflow. In such a case, a shock wave forms at the engine face and moves forward through the inlet. The engine exhaust gas temperature and mechanical speed remain constant during and after the restart cycle. However, a temporary reduction in engine fuel flow is noted. The reduction in fuel flow results from the drop in compressor discharge static pressure P_3, since the engine controller meters fuel flow proportional

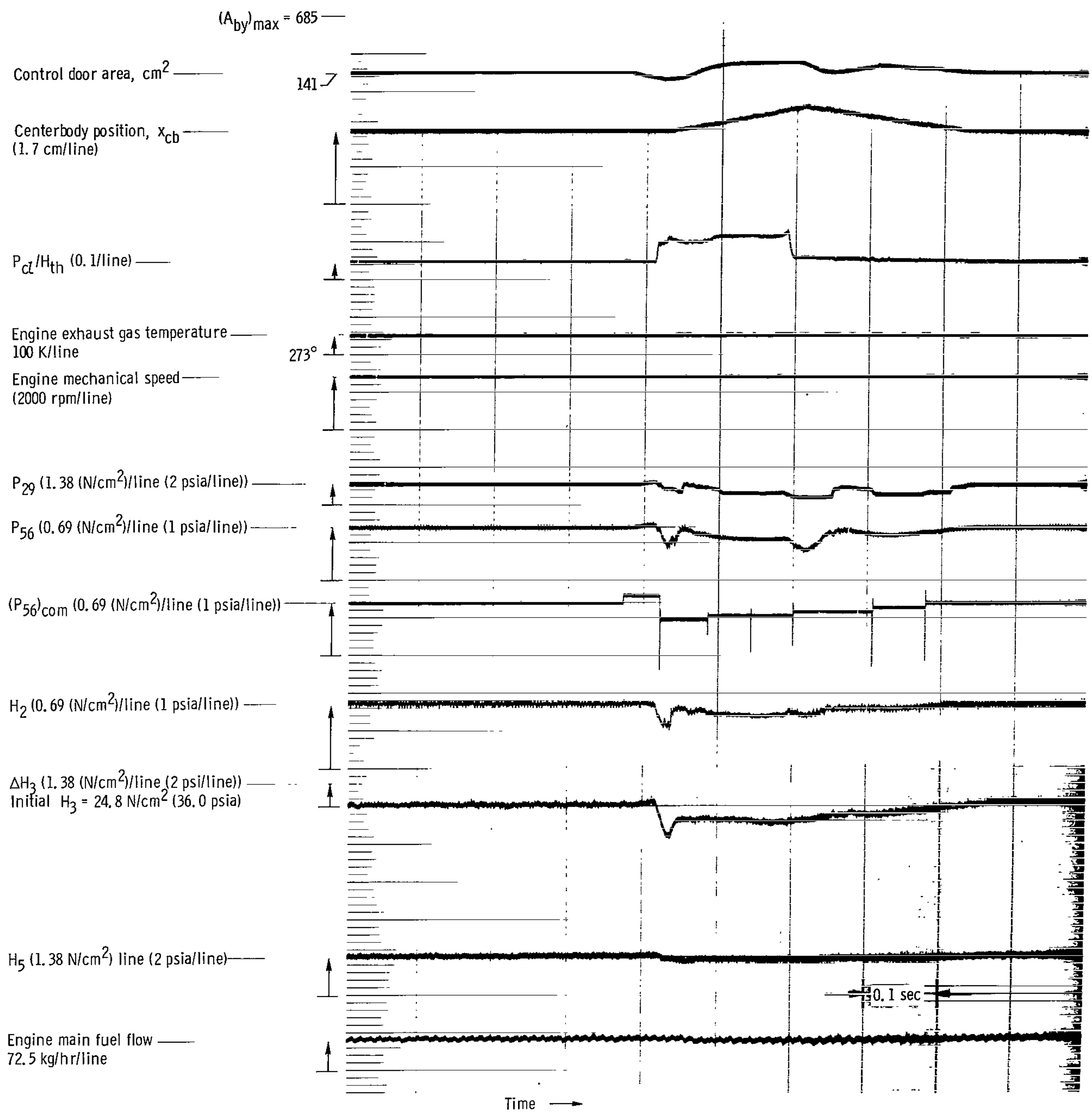

(a) Initial total pressure ratio across compressor, 4.16.

Figure 14. - Inlet unstart followed by controlled restart with J85-13 termination for various initial values of total pressure ratio across compressor. Free-stream Mach number, 2.02; free-stream temperature, 294 K; Reynolds number, 3.94×10^6; ratio of ejector bypass area to inlet capture area, 0.0257.

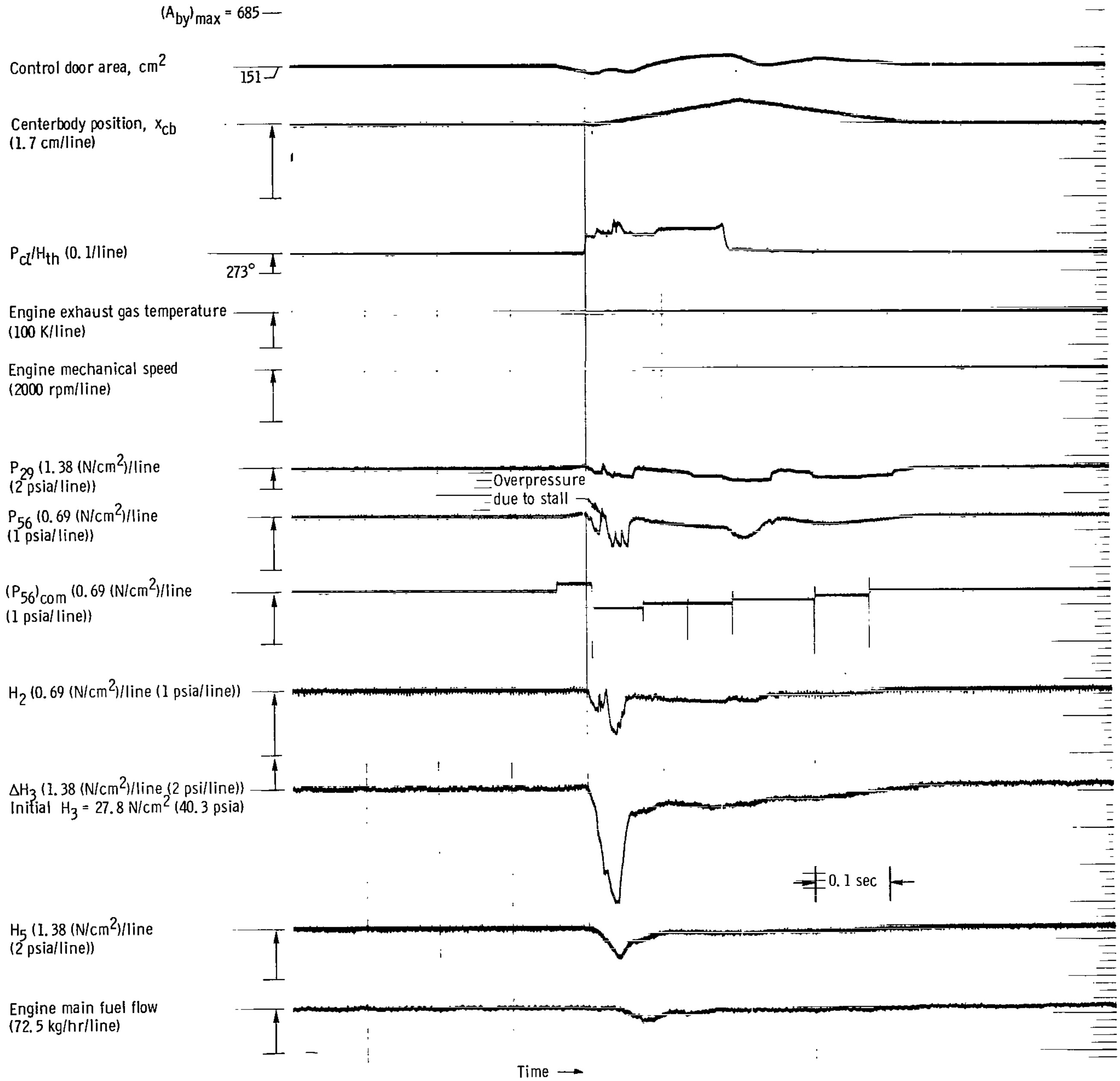

(b) Initial total pressure ratio across compressor, 4.52.

Figure 14. - Continued.

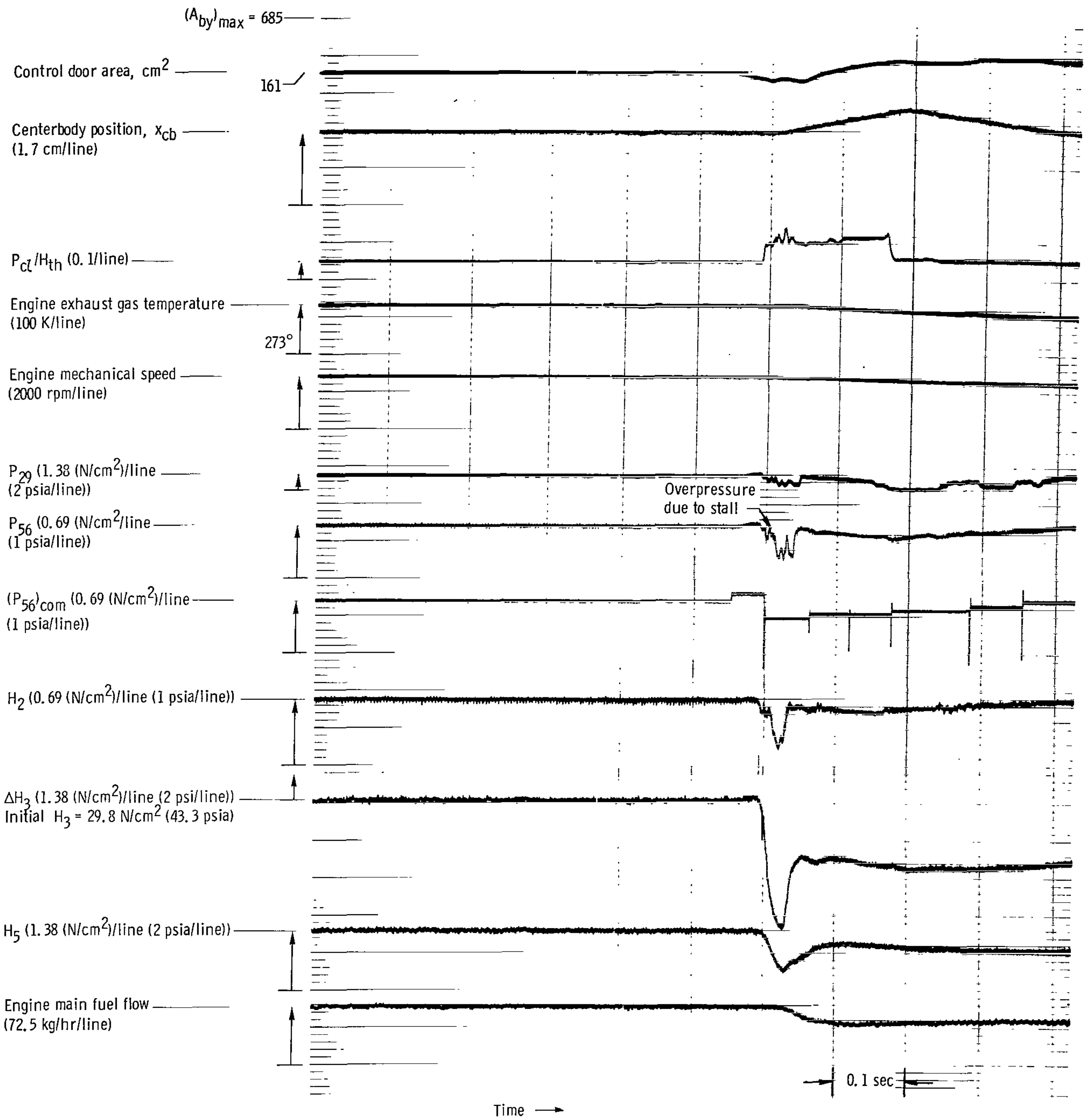

(c) Initial total pressure ratio across compressor, 4.88.

Figure 14. - Concluded.

to P_3. It is noted that after the restart cycle is completed the bypass door area has returned to the initial value. This implies that engine airflow after the restart cycle has the same value as it had before.

This combination of events implies that the compressor stalled momentarily but recovered within less than 0.1 second, that the combustor did not flame out, that the inlet restarted satisfactorily, and that afterward the engine and inlet returned to normal operation.

The final test with the engine at a free-stream Mach number of 2.02 is shown in figure 14(c). The initial H_3/H_2 value was 4.88. In this case the H_3 signal does not recover to nearly its initial value. The value of H_3/H_2 0.1 second after the unstart is approximately 3.8. The sharp spike in the upstream pressures is again present indicating the occurrence of a hammer shock. Engine exhaust gas temperature and mechanical speed decrease continuously after the unstart. Also, the bypass door area reaches a larger value after the restart cycle than before.

These events indicate that the unstart transient caused the compressor to stall and the combustor to flame out, and that the inlet restarted despite the requirement of higher bypass flow rates imposed on the inlet control system by the compressor stall.

The results of the tests at Mach 2.02 indicate that the J85-13 engine will withstand an unstart transient when operating at 86.3 percent corrected speed and at a low enough value of H_3/H_2. The possibility of compressor stall during an unstart transient increases as the steady-state value of H_3/H_2 is increased because of the engine operating nearer its stall line. No attempt was made in this program to manipulate engine parameters to minimize the possibility of compressor stall and combustor flameout, or to quickly return the engine to normal operation after these events had occurred.

The restart control test with the inlet terminated by the engine at a free-stream Mach number of 2.50 is shown in figure 15. In this test an eight-level $(P_{56})_{com}$ step schedule was used. The initial H_3/H_2 value and engine corrected speed were 4.03 and 85 percent, respectively. This value of H_3/H_2 is approximately the same as the normal operating value for that corrected speed. As in the Mach 2.02 test of figure 14(c) a decrease in both engine speed and exhaust gas temperature occurred after unstart, indicating that compressor stall and combustor flameout occurred. Preliminary analysis of unpublished data taken at Mach 2.50 during a later program at approximately the same operating conditions also indicated that combustor flameout does occur during an inlet unstart transient. Another indication of stall is the oscillatory nature of the inlet pressure traces. The peak-to-peak variations were approximately three times larger than those observed in the Mach 2.50 cold-pipe tests. This indicates that even though six bypass doors were under control as compared with three in the cold-pipe tests, the bypass area was apparently not large enough to compensate for reduced engine airflow due to

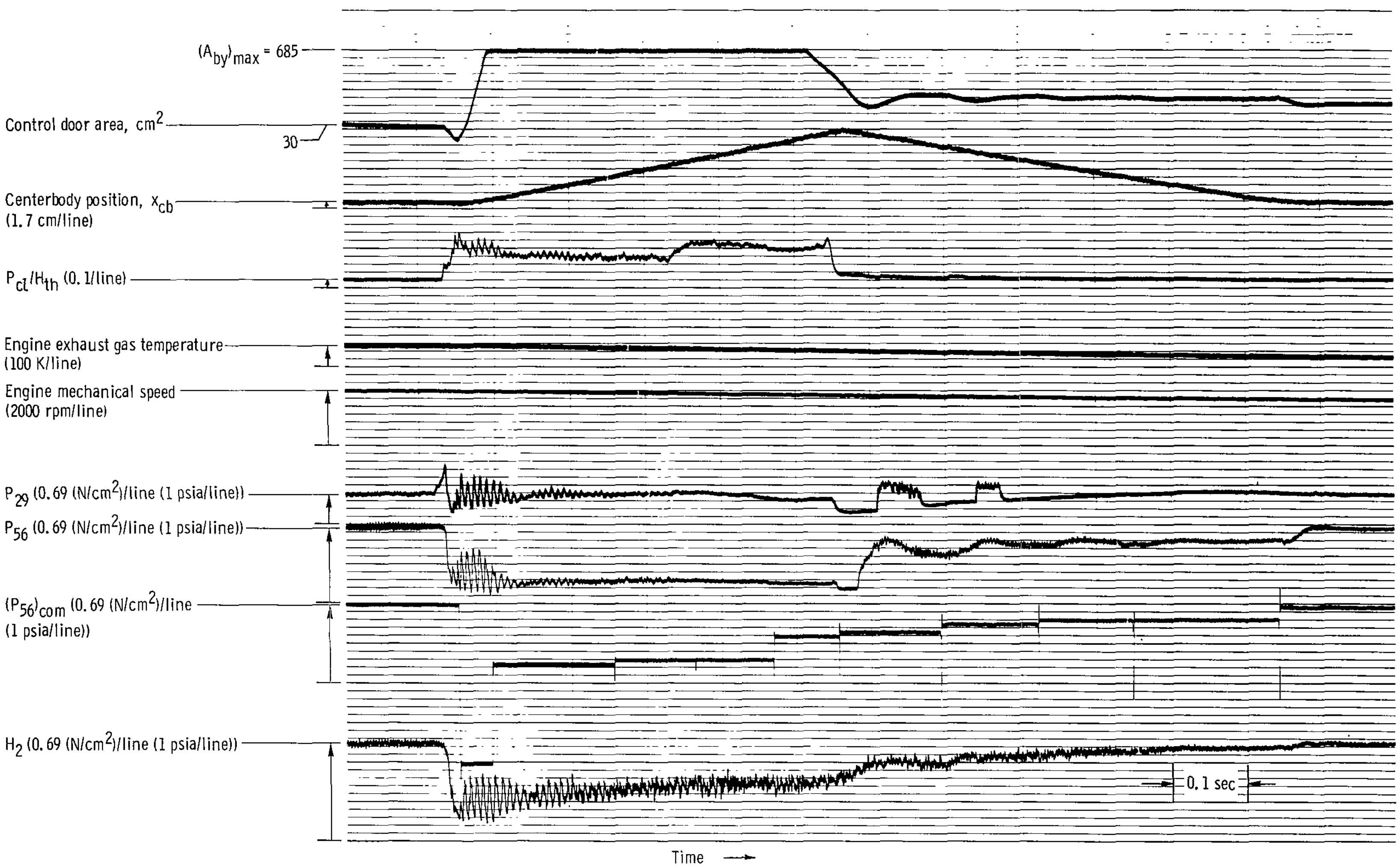

Figure 15. - Inlet unstart followed by a controlled restart with the J85-13 termination. Free-stream Mach number, 2.50; free-stream temperature, 300 K; Reynolds number, 4.30×10^6; ratio of ejector bypass area to inlet capture area, 0.0105; initial total pressure ratio across compressor, 4.03.

compressor stall and therefore resulted in mild buzz. The major portion of the oscillatory flow occurred before the bypass doors reached the maximum open position. As noted in the cold-pipe tests, the initial closure of the bypass doors after inlet unstart delays the time when the bypass doors can reach the fully open position. Although the pressure fluctuations were large, they did not upset the operation of the restart control, and the restart control returned the inlet to its initial started condition. As in the Mach 2.02 test of figure 14(c), no attempt was made to recover normal engine operation.

SUMMARY OF RESULTS

The design features and experimental performance of a control system that retains closed-loop control of terminal shock position while restarting a mixed-compression inlet were investigated. The restart control can provide significantly increased pressure recovery and reduced distortion at the compressor-face station during an inlet restart cycle as compared with a conventional control which schedules unnecessarily large bypass door areas. Inlet stability throughout restart is maintained by scheduling terminal shock control setpoint values that are high enough to assure good recovery but not high enough to cause buzz or repeated unstart. A continuous schedule of throat-exit pressure command is demonstrated to be better than a stepwise continuous schedule because it (1) permits lower distortion and higher recovery, (2) results in smooth changes in inlet pressure, and (3) results in smoother bypass servo operation.

Successful operation of the restart control system was demonstrated with the inlet coupled alternately to a cold pipe and a J85-13 turbojet engine, even in cases where compressor stall and/or combustor flameout were caused by the unstart transient. Tests of the restart control were conducted with the inlet operating at design and off-design Mach numbers. The inlet was always unstarted by a downstream disturbance. The restart control system might require some modifications to accommodate an unstart due to some types of upstream disturbances.

The terminal shock control feedback signal setpoint schedule and the unstart signal reference value had to be modified in some cases to accommodate different free-stream Mach numbers. Other changes in flight environment conditions, such as angle of attack maneuvers, might also require different control signal schedules.

Lewis Research Center,
National Aeronautics and Space Administration,
Cleveland, Ohio, September 11, 1969,
720-03.

APPENDIX - SYMBOLS

A geometric area, cm^2

A_c inlet capture area, 1760 cm^2

H absolute total pressure, N/cm^2 (psi)

$\frac{H_{max} - H_{min}}{H_2}$ distortion parameter, dimensionless

K_{56} controller gain - throat-exit static pressure feedback loop, dimensionless

K_{92} controller gain - diffuser-exit static pressure feedback loop, dimensionless

M Mach number, dimensionless

m mass-flow, kg/sec

m_0 free-stream mass-flow based on A_c, kg/sec

N engine mechanical speed, rpm

$\frac{100\left(\frac{N}{\sqrt{\theta}}\right)}{16\ 500}$ percent engine corrected speed

P absolute static pressure, N/cm^2 (psi)

R_c inlet radius at cowl lip, 23.7 cm

Re Reynolds number based on cowl-lip diameter, dimensionless

s Laplace operator

T total temperature, K

w actual engine airflow, kg/sec

$\frac{w\sqrt{\theta}}{\delta}$ engine corrected airflow, kg/sec

x location of a pressure measuring station aft of centerbody tip, cm

x_{cb} centerbody position measured forward from fully retracted location, cm

x_{cl} axial distance between cowl lip and centerbody tip, cm

ΔH_3 change in compressor discharge pressure measured from an initial steady-state condition, N/cm^2 (psi)

ΔW_d sinusoidal weight flow disturbance downstream of terminal shock, kg/sec

Δx_{cb} centerbody position measured from $M_0 = 2.50$ design position, cm